NBS TECHNICAL NOTE 933

U.S. DEPARTMENT OF COMMERCE / National Bureau of Standards

# An Infrared Technique for Heat-Loss Measurement

## NATIONAL BUREAU OF STANDARDS

The National Bureau of Standards[1] was established by an act of Congress March 3, 1901. The Bureau's overall goal is to strengthen and advance the Nation's science and technology and facilitate their effective application for public benefit. To this end, the Bureau conducts research and provides: (1) a basis for the Nation's physical measurement system, (2) scientific and technological services for industry and government, (3) a technical basis for equity in trade, and (4) technical services to promote public safety. The Bureau consists of the Institute for Basic Standards, the Institute for Materials Research, the Institute for Applied Technology, the Institute for Computer Sciences and Technology, the Office for Information Programs, and the Office of Experimental Technology Incentives Program.

**THE INSTITUTE FOR BASIC STANDARDS** provides the central basis within the United States of a complete and consistent system of physical measurement; coordinates that system with measurement systems of other nations; and furnishes essential services leading to accurate and uniform physical measurements throughout the Nation's scientific community, industry, and commerce. The Institute consists of the Office of Measurement Services, and the following center and divisions:

Applied Mathematics — Electricity — Mechanics — Heat — Optical Physics — Center for Radiation Research — Laboratory Astrophysics[2] — Cryogenics[2] — Electromagnetics[2] — Time and Frequency[2].

**THE INSTITUTE FOR MATERIALS RESEARCH** conducts materials research leading to improved methods of measurement, standards, and data on the properties of well-characterized materials needed by industry, commerce, educational institutions, and Government; provides advisory and research services to other Government agencies; and develops, produces, and distributes standard reference materials. The Institute consists of the Office of Standard Reference Materials, the Office of Air and Water Measurement, and the following divisions:

Analytical Chemistry — Polymers — Metallurgy — Inorganic Materials — Reactor Radiation — Physical Chemistry.

**THE INSTITUTE FOR APPLIED TECHNOLOGY** provides technical services developing and promoting the use of available technology; cooperates with public and private organizations in developing technological standards, codes, and test methods; and provides technical advice services, and information to Government agencies and the public. The Institute consists of the following divisions and centers:

Standards Application and Analysis — Electronic Technology — Center for Consumer Product Technology: Product Systems Analysis; Product Engineering — Center for Building Technology: Structures, Materials, and Safety; Building Environment; Technical Evaluation and Application — Center for Fire Research: Fire Science; Fire Safety Engineering.

**THE INSTITUTE FOR COMPUTER SCIENCES AND TECHNOLOGY** conducts research and provides technical services designed to aid Government agencies in improving cost effectiveness in the conduct of their programs through the selection, acquisition, and effective utilization of automatic data processing equipment; and serves as the principal focus wthin the executive branch for the development of Federal standards for automatic data processing equipment, techniques, and computer languages. The Institute consist of the following divisions:

Computer Services — Systems and Software — Computer Systems Engineering — Information Technology.

**THE OFFICE OF EXPERIMENTAL TECHNOLOGY INCENTIVES PROGRAM** seeks to affect public policy and process to facilitate technological change in the private sector by examining and experimenting with Government policies and practices in order to identify and remove Government-related barriers and to correct inherent market imperfections that impede the innovation process.

**THE OFFICE FOR INFORMATION PROGRAMS** promotes optimum dissemination and accessibility of scientific information generated within NBS; promotes the development of the National Standard Reference Data System and a system of information analysis centers dealing with the broader aspects of the National Measurement System; provides appropriate services to ensure that the NBS staff has optimum accessibility to the scientific information of the world. The Office consists of the following organizational units:

Office of Standard Reference Data — Office of Information Activities — Office of Technical Publications — Library — Office of International Standards — Office of International Relations.

---

[1] Headquarters and Laboratories at Gaithersburg, Maryland, unless otherwise noted; mailing address Washington, D.C. 20234.

[2] Located at Boulder, Colorado 80302.

# An Infrared Technique for Heat-Loss Measurement

technical note, no.


D.M. Burch, T. Kusuda,
and D.G. Blum

Building Environment Division
National Bureau of Standards
Washington, D.C. 20234



Prepared for

Federal Energy Administration
Washington, D.C. 20461

U.S. DEPARTMENT OF COMMERCE, Juanita M. Kreps, Secretary

Dr. Betsy Ancker-Johnson, Assistant Secretary for Science and Technology
U.S. NATIONAL BUREAU OF STANDARDS, Ernest Ambler, Acting Director

Issued April 1977

National Bureau of Standards Technical Note 933
Nat. Bur. Stand. (U.S.), Tech. Note 933, 52 pages (April 1977)
CODEN: NBTNAE

U.S. GOVERNMENT PRINTING OFFICE
WASHINGTON: 1977

For sale by the Superintendent of Documents, U.S. Government Printing Office
Washington, D.C. 20402 - Price $1.10

Stock No. 003-003-01746-9

## CONTENTS

## NOMENCLATURE

| | |
|---|---|
| A | Surface area |
| $C_f$ | Fraction of energy emitted from front side |
| $C_p$ | Constant-pressure specific heat |
| d | Spacing between heating elements |
| E | Total thermal radiation leaving a surface |
| Fo | Fourier modulus, $Fo = \tau/(\rho \cdot L \cdot C_p/h)$ |
| h | Heat-transfer coefficient |
| H | Biot number, $H = h_f \cdot d^2/k \cdot L$ |
| I | Electric current or isotherm level |
| k | Thermal conductivity |
| L | Thickness |
| m | Heat generation rate per unit length |
| p | Rate of internal heat generation per unit volume |
| q | Heat-flux rate |
| r | Object distance |
| s | Edge length of square |
| t | temperature |
| T | Absolute temperature, $T = t + 459.7$ |
| V | Voltage |
| x | distance |
| Z | Transfer function for IR camera |

## Greek Symbols

| | |
|---|---|
| $\alpha$ | Angle subtended by edge of square |
| $\theta$ | Dimensionless temperature, $\theta = (t - t_a)/(p \cdot L/h_f)$ |
| $\varepsilon$ | Emissivity |
| $\eta$ | Dimensionless distance, $\eta = x/d$ |
| $\tau$ | Time |
| $\rho$ | Density |
| $\sigma$ | Stefan-Boltzmann constant |
| $\upsilon$ | Dimensionless temperature, $\upsilon = (t - t_a)/(m \cdot d/L \cdot k)$ |

## SUBSCRIPTS

| | |
|---|---|
| a | Ambient surroundings |
| b | Back side |
| f | Front side |
| h | Hemispherical property |
| i | Initial |
| n | Normal property |
| R | Heat-flow reference pad |
| s | Building surface |

Conversion Factors to Metric (S.I.) Units

| Physical quantity | Symbol | To Convert from | To | Multiply by |
|---|---|---|---|---|
| Length | $x$ | ft | m | .305 |
| Area | $A$ | $ft^2$ | $m^2$ | $9.29 \times 10^{-2}$ |
| Volume | | $ft^3$ | $m^3$ | $2.83 \times 10^{-2}$ |
| Temperature | $t$ | Fahrenheit | Celsius | $t_c=(t_f-32)/1.8$ |
| Absolute temperature | $\underset{\cdot}{T}$ | Rankine | Kelvin | 0.556 |
| Temperature difference | $\Delta t$ | Fahrenheit | $\Delta K$ | 0.556 |
| Mass | | lb | kg | 0.454 |
| Density | $\rho$ | $lb/ft^3$ | $kg/m^3$ | $1.602 \times 10^1$ |
| Thermal conductivity | $k$ | Btu/h·ft·F | W/m·k | 1.73 |
| Heat-flow rate | | Btu/h | W | .293 |
| Heat-flux rate (or self-emitted radiation) | $q$ <br> $E$ | $Btu/h \cdot ft^2$ | $W/m^2$ | 3.153 |
| Specific heat | $C_p$ | Btu/lb·F | J/kg·k | $4.187 \times 10^3$ |

# AN INFRARED TECHNIQUE FOR HEAT-LOSS MEASUREMENT

By

D. M. Burch, T. Kusuda, and D. G. Blum

This paper describes a newly developed technique for estimating heat-loss rate utilizing an infrared television system. A device called a heat-flow reference pad was developed that makes it possible to estimate quantitatively the heat-loss rate at the surface of a building without the need for a conventional heat-flow meter to be mounted on the surface. Technical considerations for the design of a heat-flow reference pad are presented. The infrared measurement technique predicted heat-loss rates in the laboratory and field within approximately 12%.

Key words: Heat-flow measurements; infrared heat-loss measurement technique; measurement technology; thermography.

## 1. INTRODUCTION

With the increasing scarcity of domestic energy resources and increasing cost of fuel for heating and cooling buildings, better insulation of walls and roofs has become both a national goal and a matter of financial concern to home and building owners. Since the presence of insulation and the quality of workmanship used in its installation are generally not visible, compliance with specifications and code provisions is not easily ascertainable by conventional means. Therefore, at the request and under sponsorship of the Federal Energy Administration, NBS has conducted research to develop an infrared television technique for evaluating the heat-loss characteristics of completed buildings, walls, and roofs.

An infrared television system senses the total thermal radiation emitted and reflected from a surface. A thermal picture is produced on a television screen in which the level of gray tones approximately corresponds to surface temperature. Since such a system essentially produces a temperature profile map of a surface, it is an effective tool for locating and identifying major heat leaks of buildings [1,2,3]*. In a recent study [4] conducted at the National Bureau of Standards, it was shown that infrared (IR) thermography could be used as a survey technique to distinguish between insulated and non-insulated wood-frame cavity walls.

This research was supported by the Federal Energy Administration.
* Figures in brackets indicate the literature references at the end of this paper.

Recently there has been much interest in developing an IR measurement technique that would permit the measurement of heat-loss rates from the surfaces of buildings. The development of such a technique would make it possible to conduct surveys of the side walls of residences in order to evaluate their heat-loss characteristics. Another application for the IR heat-loss measurement technique would be to obtain a heat-loss profile map of a built-up roofing system, thereby permitting regions having wet insulation to be located. These regions would have higher heat-loss rates than regions having dry insulation.

Previous attempts to quantitatively measure heat-loss rates using IR thermography have been frustrated by the difficulty of converting surface temperatures into corresponding heat-loss rates. To perform this conversion, a heat-transfer coefficient which depends on the convective air movement at the surface as well as the radiation heat transfer with surrounding surfaces must be accurately specified. The radiation exchange is in turn a complex function of the emissivity of the surface, geometric view factor, and the temperature of the surrounding surfaces. The inability to know all of these factors with certainty makes it extremely difficult to predict accurately the heat-transfer coefficient.

The purpose of the present paper is to present preliminary findings of a study to develop an IR measurement technique. A device called a heat-flow reference pad (HFRP), was developed that makes it possible to estimate the heat-loss rate through the exterior surface of a building.

The procedure for performing a heat-loss measurement at the surface of a building is as follows: Both the building surface and the HFRP are included in the thermal picture of an IR television system. The front-side heat flux of the HFRP is adjusted until it appears the same as the building surface in the thermal picture. The front-side heat flux is adjusted by varying the electric power supplied to the device. At this condition, the heat-loss rate from the HFRP will be very nearly equal to the heat-loss rate from the building surface, providing the emissivity and surface air velocity of the HFRP and the building surface do not differ significantly.

The IR heat-loss measurement technique has several advantages over conventional heat-flow transducers for measuring surface heat-loss rates. When using the IR heat-loss measurement technique it is not necessary for a measuring transducer to touch the surface; therefore, the original heat-flow rate is not disturbed. This feature becomes a significant advantage when measuring the heat-loss rates through a building surface having a low thermal resistance. Another advantage of the IR heat-loss measurement technique is that it can provide a heat-flow profile map of a building surface, providing that the emissivities of the components that comprize the building surface are essentially the same. When a surface of a building has a wide variation of heat-loss rate, many conventional heat-flow transducers are required to determine the heat flow pattern.

## 2. DESCRIPTION OF INFRARED TELEVISION SYSTEM

A photograph of the IR television system used with the HFRP to measure surface heat-flow rates is shown in figure 1. The equipment from right to left consists of IR television camera, the black and white television monitor, the color television display, and the temperature profile adapter. The thermal radiation that is emitted and reflected from a surface is sensed by the IR camera and converted into a video signal. The IR camera consists of an optical scanning system with a liquid-nitrogen-cooled indium-antimonide photovoltaic detector having high sensitivity in the spectral range 2.0 to 5.6 micrometers.

The video signal from the IR camera is processed in the black and white television monitor, where it is converted into a thermal picture in which the gray tones of the picture directly relate to surface temperatures. This thermal image is displayed on a television screen which may be photographed with a conventional camera. The video signal is also fed into the color television display where the temperature range has been subdivided into ten regions, each color-coded with a separate color. The temperature profile adapter selects a single horizontal trace line* of the thermal picture of the black and white television monitor and displays this line such that the temperature change throughout the line is approximately represented as a vertical displacement.

## 3. DESCRIPTION OF HEAT-FLOW REFERENCE PAD

In designing a heat-flow reference pad it is necessary to consider the following features and factors:

- Uniform front-side heat flux with small edge effects.
- Fast response time.
- Small back-side losses.
- Sufficient size to permit its surface temperature to be resolved by IR television camera.
- Measurement error that occurs when the emissivity of the HFRP is different from that of the building surface.
- Measurement error that occurs when the convective heat transfer at the surface of the HFRP is different from that at the building surface.
- Measurement error due to the minimum detectable temperature difference of the IR camera.

A major source of uncertainty in the IR technique for heat-loss measurement is the minimum detectable temperature difference of the IR camera, which determines the precision to which the radiance level of the HFRP can be adjusted to the level of a building surface. It is shown in the appendix that, when emittance and rate of convective heat transfer for both the HFRP and the building surface are identical, the measurement

---

* The thermal picture consists of a series of consecutive horizontal trace lines displayed on a cathode-ray tube.

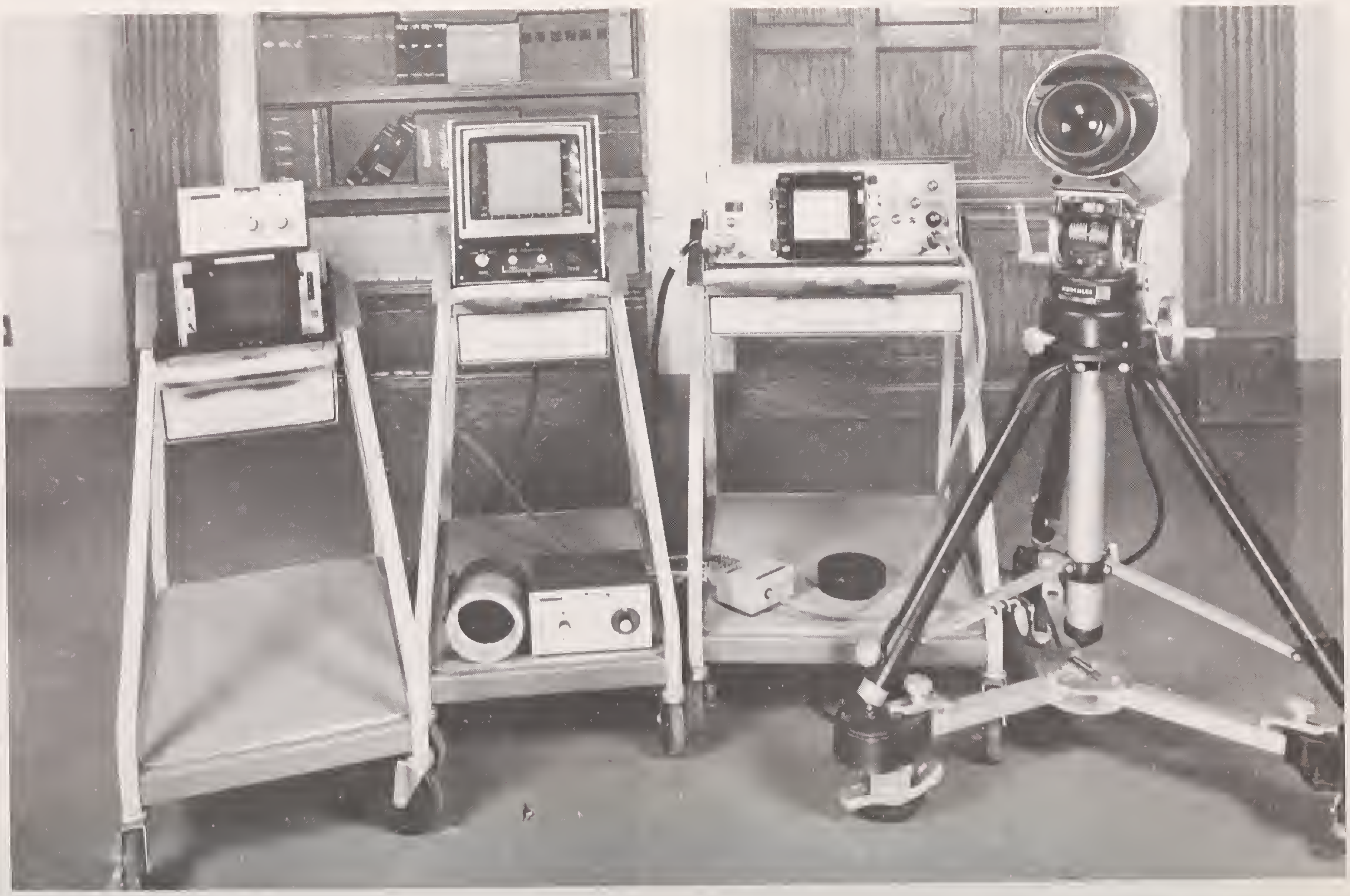

Figure 1. Infrared television system.

error is given by $\Delta T_m/(T_s - T_a)$, where $\Delta T_m$ is the minimum detectable temperature difference and $(T_s - T_a)$ is the surface-to-air temperature difference at the building surface. When the rate of convective heat transfer is large or the heat-loss rate at the building surface is small, the surface-to-air temperature difference becomes small and the uncertainty in the heat-loss measurement becomes large. For instance, it was shown that for a 15-mph wind condition the measurement error could be as high as 48 percent for an insulated wood-frame wall. However, under still-air conditions, the measurement error due to minimum detectable temperature difference was shown to be less than 12 percent.

Other factors which cause measurement error are departures of the rate of convective heat transfer and emittance for the HFRP from that of the building surface. It is shown in the appendix that under still air conditions, when the convective air movement at the surfaces of the heat-flow reference pad and building surface are very likely to be approximately the same, the error due to differences in emissivity will usually be less than 5 percent. On the other hand, when measurements are performed under high wind conditions, precautions need to be taken to insure that both the building surface and the HFRP are exposed to the same convective conditions, in order to obtain accurate measurements. It is shown in the appendix that exposure of the HFRP to a 30-percent greater convective heat-transfer condition could result in a measurement error of approximately 19 percent.

A prototype heat-flow reference pad was constructed. The device, shown in figure 2, consists of a thin-foil heater, having a thickness of 72 mils, spot-glued to a 3.875-inch thick polystyrene insulating board (2 x 2 ft). The heater (10.87 x 10.59 in) contains electric heating elements spaced 0.147 inch on center (see figure 3). The front-side surface of the heater was spray-painted with two layers of matt-black paint having an emissivity of approximately 0.96.

A schematic of the control and measurement system used to adjust and measure the electric power delivered to the HFRP is shown in figure 4. A variable-voltage D.C. power supply delivers electric power to the HFRP. When the switch is in the left position, the D.C. voltmeter measures the voltage drop across the thin-foil heater. When the switch is in the right position, the D.C. voltmeter measures the voltage drop across the 80-ohm resistor, permitting the current to the thin-foil heater to be calculated from Ohm's law.

Two methods were used to determine the front-side heat flux for the HFRP. The first method, voltage (V) and current (I) supplied to the HFRP were measured and the front-side heat flux (q) was determined from the relation:

$$q = C_f \cdot V \cdot I/A \qquad (1)$$

where $C_f$ is the fraction of the electric power input to the HFRP that appears as front-side heat flux, after a steady-state condition has been

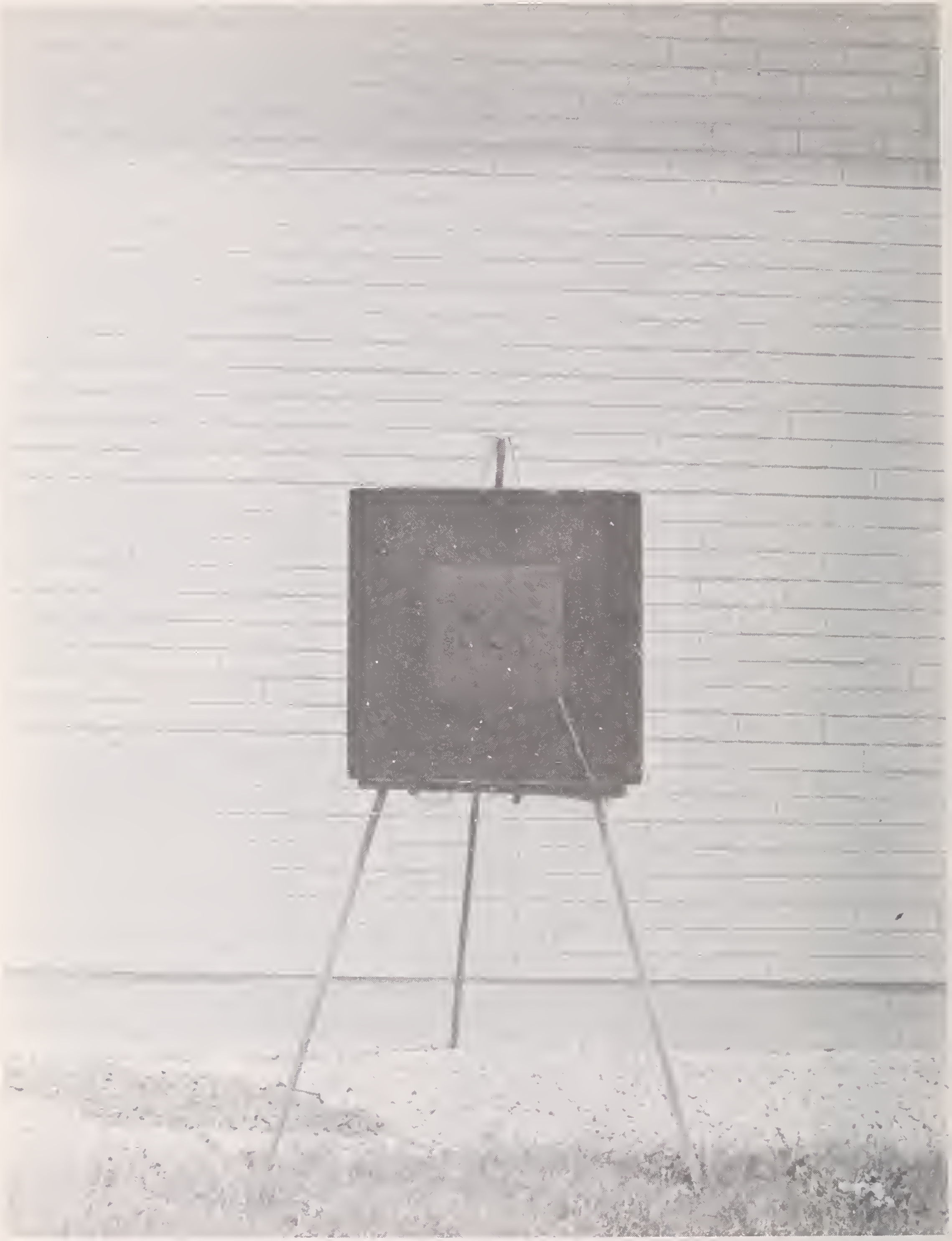

Figure 2. Experimental prototype heat-flow reference pad.

reached. The factor $C_f$ is determined by subtracting the back-side losses from the total power input and dividing by the total power input. The surface area of the thin-foil heater is denoted by A. One problem encountered in using this method was that the back-side losses varied as a function of time with a rather long time constant, requiring a long time to complete the successive adjustments of the HFRP.

The second method of measuring the front-side heat flux was to use three heat-flow meters that were spot-glued in a horizontal line across the thin-foil heater. Each heat-flow meter consisted of a 2.0-inch diameter, 0.13-inch thick, circular disk made of polyvinylchloride filler material, having an embedded thermopile. The millivolt signal generated by the thermopile is proportional to the heat flow through the circular disk. The heat-flow meters were calibrated in an 8-inch guarded-hot-plate apparatus conforming with the requirements of ASTM Standard Method of Test C 177-71 [5]. These three heat-flow meters were connected in series. The presence of these heat-flow meters has a very small effect on the original heat-flow pattern of the HFRP owing to the large thermal resistance of the back-side insulating board. Heat-flow rates measured with these heat-flow meters were not corrected for the thermal resistance of heat-flow meters.

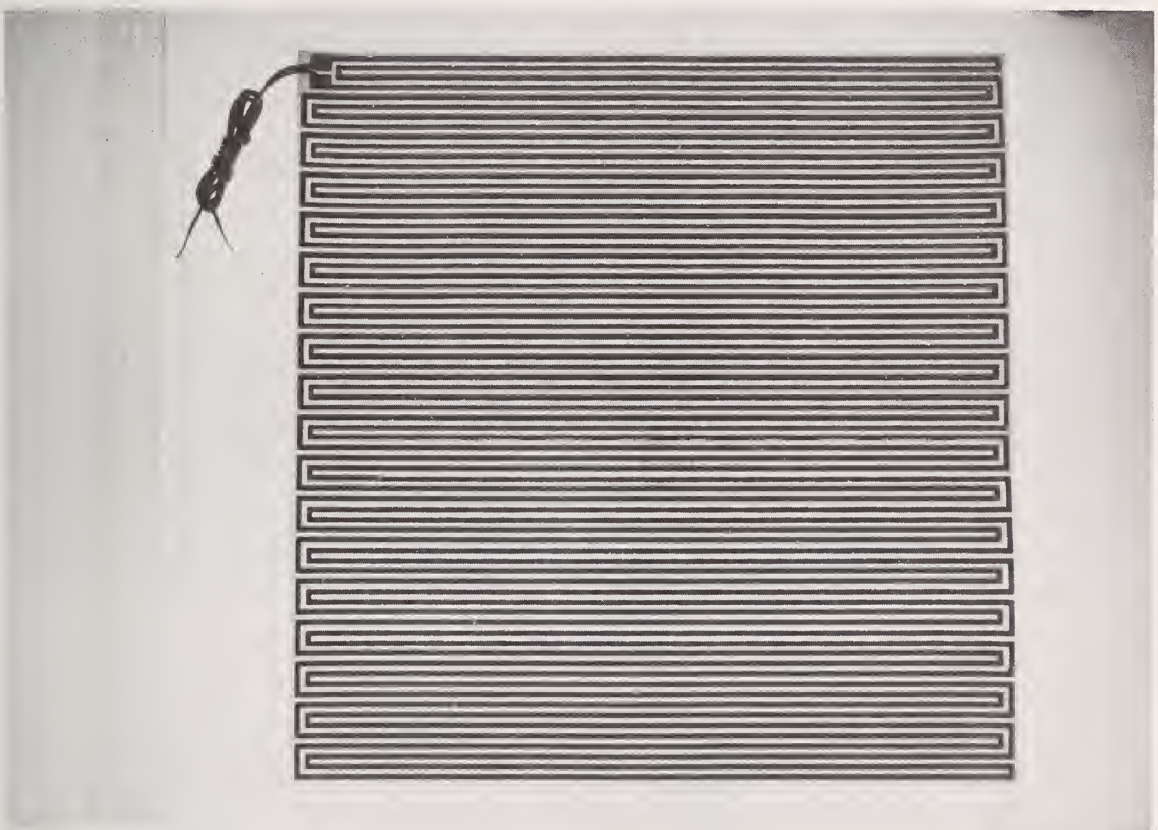

Figure 3. Thin-foil heater.

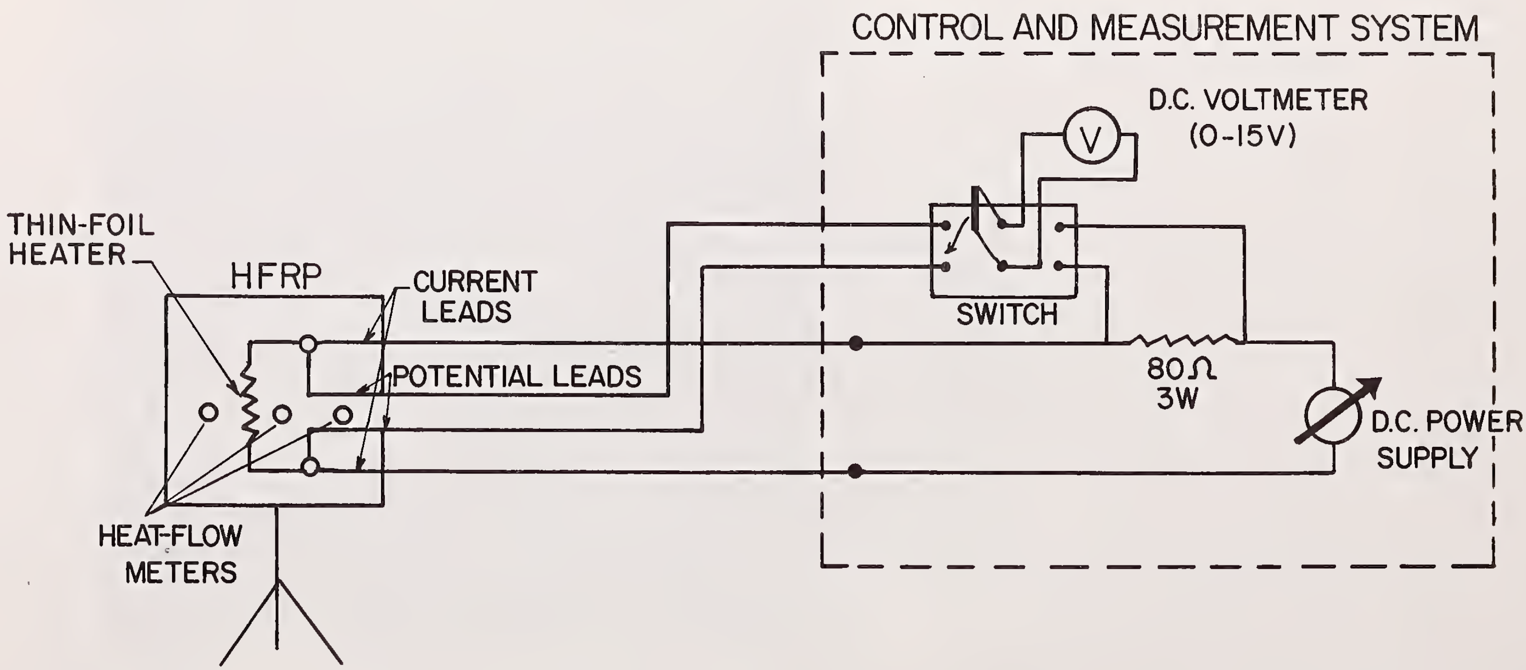


Figure 4. Schematic of control and measurement system.

## 4. LABORATORY HEAT-LOSS MEASUREMENTS

Known heat-loss rates were produced in the laboratory and were measured by the IR heat-loss measurement technique. In creating laboratory heat-loss rates, values were selected that were representative of heat-loss rates through the walls of actual buildings.

A schematic of the apparatus for producing known heat-loss rates is shown in figure 5. The device consisted of a small wooden rectangular enclosure (1.51 x 1.51 x 2 ft). One face of the enclosure contained a wooden frame that supported a piece of polystyrene insulating board of known thickness. An 8-junction copper-constantan thermopile was installed across the insulating board as shown in figure 5. The exterior surface of the insulating board was spray-painted with two layers of matt-black paint having emissivity of approximately 0.96. An electric heater and fan were installed inside the box as shown in figure 5. Various heat-flow rates through the insulating board were created in the laboratory by varying the electric power supplied to the heater. Edge losses from the insulating board were assumed to be negligibly small, since the thermopile was located a distance from the edge equivalent to four thicknesses of the insulating board.

The thermal conductivity of the insulation board was measured with the guarded-hot-plate apparatus in accordance with ASTM Standard Method of Test C 177-71 [5] and found to be 0.270 $Btu \cdot in/h \cdot ft^2 \cdot F$. The thickness of the board was measured and found to be 0.703 inch. The heat-flow rate is related to the temperature difference across the insulating board by the relation:

$$q/A = k \cdot \Delta t / L \qquad (2)$$

where

$q/A$ = heat-transfer rate, $Btu/h \cdot ft^2$ ($W/m^2$)
$k$ = thermal conductivity, $Btu/h \cdot ft \cdot F$ ($W/m \cdot K$)
$\Delta t$ = temperature difference, F (K)
$L$ = thickness, ft (m)

Substituting the above values into equation (2), the heat flux is given by the relation, $q/A = 0.384 \cdot \Delta T$. The foregoing equation assumes that the heat transfer in the vicinity of the thermopile is one-dimensional.

The heat-loss rate of the insulating board was also measured with a calibrated heat-flow meter similar to the one used on the HFRP. This heat-flow meter was spot-glued at the center of the exterior surface of the insulating board. Signals recorded from this heat-flow meter were observed to contain fluctuations due to convective air movements. Therefore, this heat-flow meter was only used as a back-up measurement for the thermopile heat-loss measurement. The heat-flow meter itself

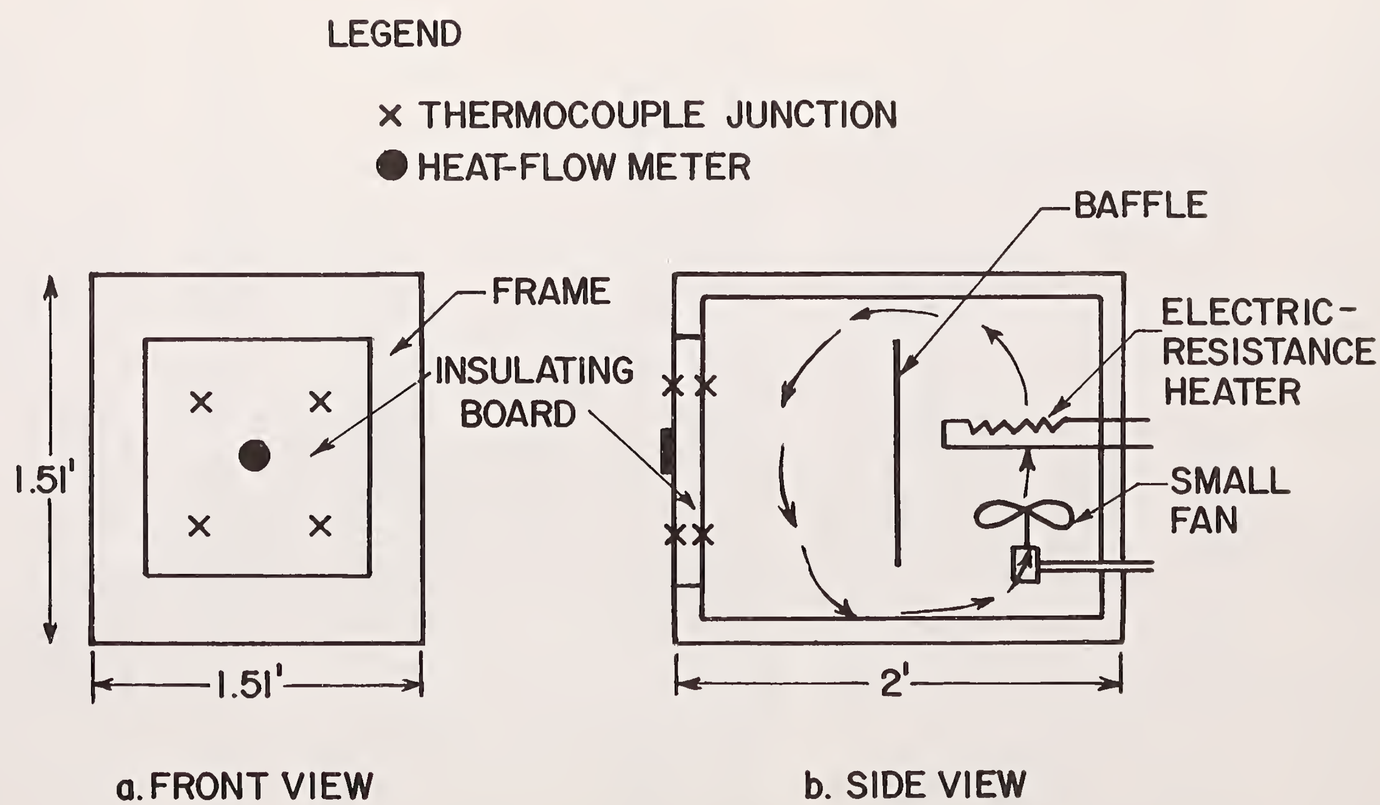


Figure 5. Apparatus for producing known heat-flow rates in the laboratory.

had a small effect on disturbing the original heat-flow pattern, since its thermal resistance was approximately 0.03 times that of the heat-flow path through the insulating board. Heat-flow rates measured with the heat-flow meter were not corrected for the thermal resistance of the heat-flow meter.

It was found that the greatest sensitivity (ability of the IR television system to detect temperature difference) could be attained when the temperature-profile adapter of the IR television system was used. In conducting an IR heat-loss measurement, the procedure used was to pass the single trace line displayed on the temperature-profile adapter through the image of both the HFRP and the apparatus for producing known heat-flow rates. The front-side heat-flux rate of the HFRP was adjusted until the vertical displacement of the trace line was the same for both the reference pad and the apparatus. A photograph of the cathode-ray tube of the temperature profile adapter at the conclusion of an IR heat-loss measurement is shown in figure 6.

Comparisons of actual heat-flow rates created by the apparatus of figure 5 and corresponding measured values using the IR heat-loss measurement technique are given in tables 1 and 2. For the measurements of table 1 the front-side heat flux of the HFRP was predicted from its electric power input rate and the calculated reverse-side heat loss, whereas for the measurements of table 2 the front-side heat flux was determined by using three heat-flow meters attached to the HFRP.

When the front-side heat flux of the HFRP was determined by measuring the electric power delivered to the HFRP (table 1), the accuracy of the IR heat-loss measurement technique was found to be within approximately 10%. The table indicates a tendency for the heat-loss values determined from the IR heat-loss measurement technique to be higher than corresponding measured values, due to the fact that insufficient time was allowed to attain a steady-state condition. Initially a significant portion of the electric power input to the HFRP appears as back-side losses. The transient back-side loss requires a long time interval to decay to a small steady-state value.

When the front-side heat-flux rates of the HFRP were determined by the three heat-flow meters (table 2), predicted heat-flow rates determined by the IR heat-loss measurement technique were within approximately 6 percent of measured values.

## 5. FIELD HEAT-LOSS MEASUREMENTS

The IR heat-loss measurement technique was used to measure the heat-loss rate at the exterior wall surface of Building 226 at NBS. The wall was constructed of fire-clay brick having an emissivity of approximately 0.94 (see table A-1 in the appendix). It should be pointed out that the particular wall studied was the rear wall of a recessed loading

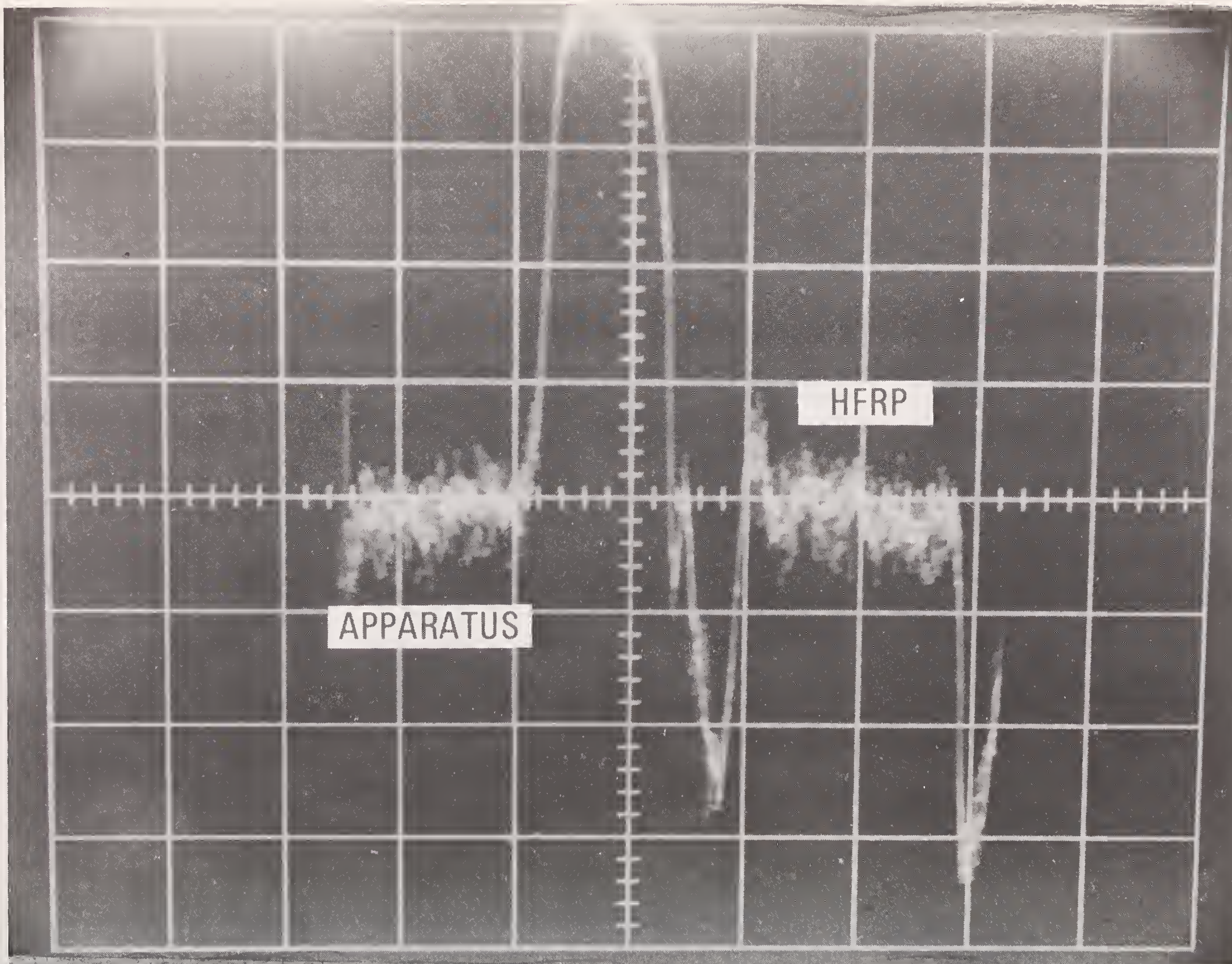


Figure 6. Cathode-ray tube of temperature-profile adapter at the conclusion of an IR heat-loss measurement.

TABLE 1

Laboratory Heat-Flow Measurements

(By measuring electric energy delivered to HFRP)

| Test No. | Heat-Flow Rate, Btu/h·ft$^2$ | | | Error* % |
|---|---|---|---|---|
| | Surface | | Heat-Flow Reference Pad | |
| | Thermopile | Heat-Flow Meter | | |
| 1 | 1.90 | 2.13 | 2.06 | + 8.4 |
| 2 | 3.84 | 3.82 | 3.72 | - 3.1 |
| 3 | 4.84 | 4.73 | 5.27 | + 8.9 |
| 4 | 6.78 | 6.67 | 7.47 | +10.2 |

* HFRP with respect to thermopile heat-flow measurements

TABLE 2

Laboratory Heat-Flow Measurements

(Using Heat-Flow Meters on HFRP)

| Test No. | Heat-Flow Rate, $Btu/h \cdot ft^2$ | | | Error** % |
|---|---|---|---|---|
| | Surface | | Heat-Flow Reference Pad | |
| | Thermopile | Heat-Flow Meter | | |
| 1 | * | 2.13 | 2.04 | 4.2*** |
| 2 | 2.21 | 2.42 | 2.08 | -5.9 |
| 3 | 1.76 | 1.84 | 1.79 | +1.7 |
| 4 | 4.10 | 4.01 | 4.01 | -2.2 |
| 5 | 4.68 | 4.69 | 4.89 | +4.5 |
| 6 | 5.88 | 5.75 | 6.20 | +5.4 |

* Data not available.

** HFRP with respect to surface heat-flow rate determined with thermopile.

*** HFRP with respect to surface heat-flow rate determined with heat-flow meter.

platform, so that the surface being investigated was partly protected from wind gusts. A photograph showing the experimental set-up for the field heat-loss measurement is shown in figure 7.

The thick heat-flow meter that was attached to the HFRP for the present study had a thermal time constant of approximately 15 minutes and required considerable time to reach a steady-state condition. For the final prototype HFRP, it is recommended that this heat-flow meter be very thin and thereby have a small time constant.

Upon moving into the field, it was observed that the measured heat-loss rate through the building wall and the HFRP contained rather large fluctuations due to convective air movements at the exterior surface. It was, therefore, necessary to feed the signals from both the heat-flow meter mounted on the building surface and the three series-connected heat-flow meters attached to the HFRP into strip-chart recorders. Figure 8 shows variation in signal observed from the heat-flow meters of the HFRP. It is recommended that the final prototype HFRP be used with an analog integrator for averaging the signal from the heat-flow meters of the HFRP. Similar variations in heat-flow rate were observed by use of the heat-flow meter attached to the building wall.

For the field heat-loss measurements, the front-side heat flux of the HFRP was determined by using the heat-flow meters. A comparison of measured wall heat-loss rates and corresponding values determined by the IR heat-loss measurement technique is given in table 3.

TABLE 3

Field Heat-Flow Measurements*

| Test No. | Heat-Flow Rate, Btu/h·ft$^2$ | | Error % |
|---|---|---|---|
| | Wall | HFRP | |
| 1 | 5.1 | 5.7 | +11.6 |
| 2 | 5.5 | 6.1 | +10.9 |
| 3 | 6.3 | 6.2 | - 1.6 |

*using heat-flow meters attached to HFRP

At the time of the field and laboratory measurements, the authors were unaware of the very long period required for the heat-flow meters of the HFRP to reach a steady-state condition. Much of the error for test numbers 1 and 2 of table 3 was believed to be due to the existence of non-steady conditions. During the initial successive adjustments of the HFRP, the front-side heat flux of the HFRP was increased in a stepwise fashion. The temperature difference across the heat-flow meters is initially large and decays slowly to a reduced steady-state value. For test number 3, it was believed that sufficient time had elapsed for a near steady-state condition to be attained.

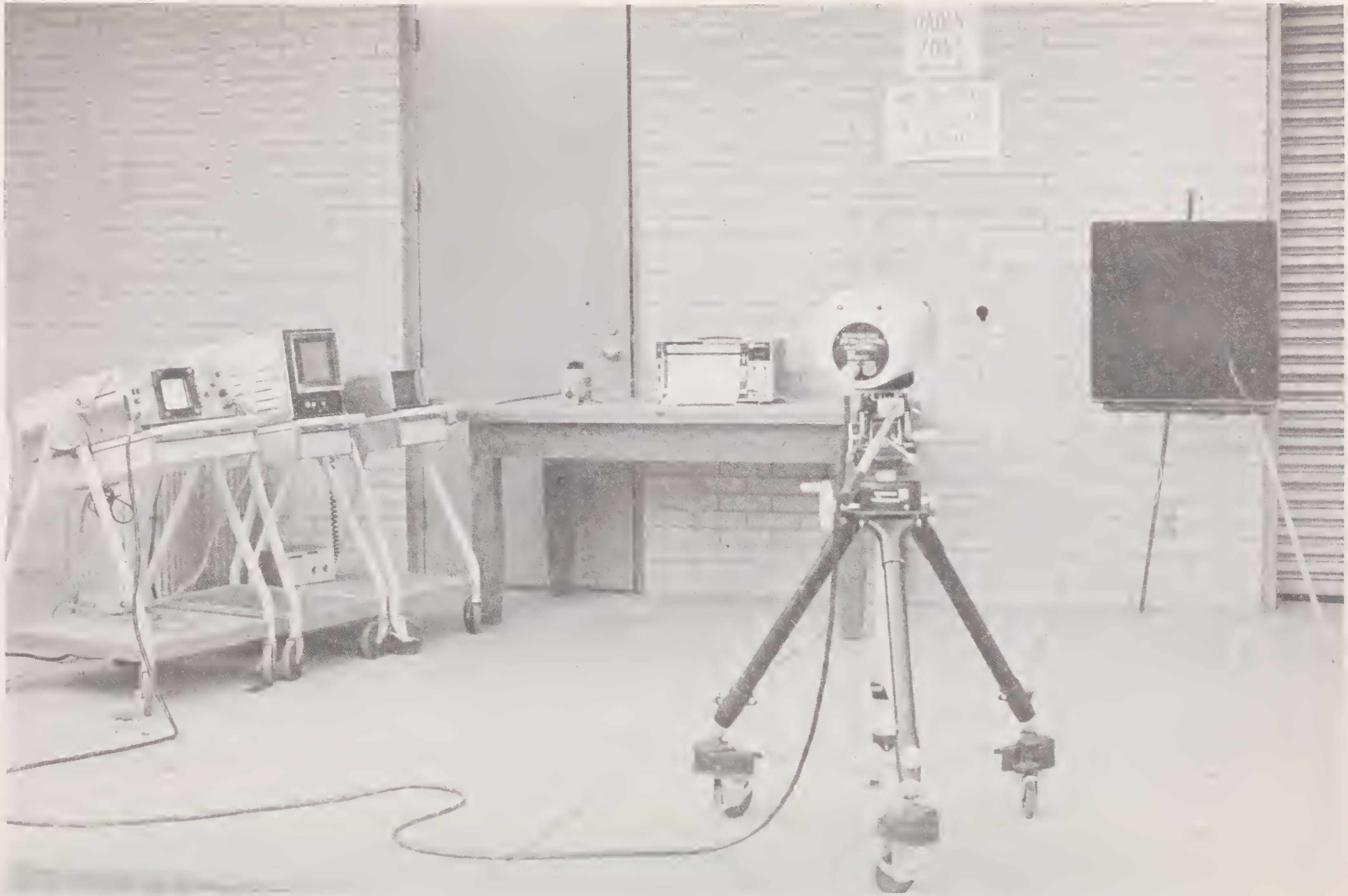

Figure 7. Experimental set-up for field heat-loss measurements.

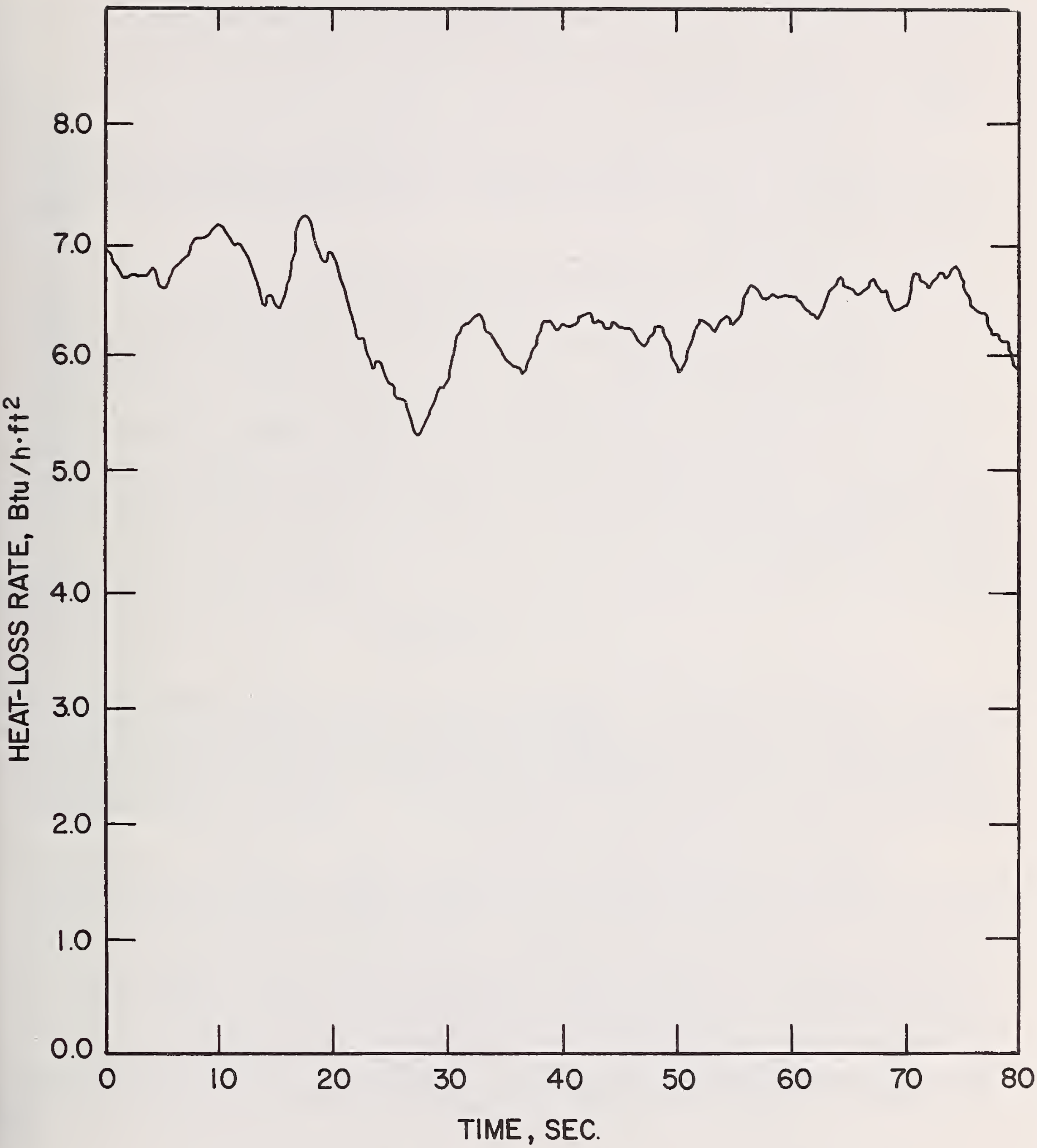


Figure 8. Variations in signal observed from the heat-flow meters of the HFRP.

For the laboratory measurements presented in the previous section, still-air conditions were present. Errors due to surface convective heat transfer were probably small. However, for the field measurements, some differences in convective heat transfer at the surfaces of the HFRP and the building surface may have existed, thereby giving rise to measurement error. Air velocities at these surfaces were not measured, so it was not possible to investigate errors due to differences in surface convective heat transfer.

Of particular importance is the time required to perform a heat-loss measurement using the IR technique. For a final prototype HFRP (one utilizing a fast heat-flow meter), the total measurement time would include the following:

- successive adjustments of HFRP $\sim$ 5 minutes
- conditioning period for heat-flow meter to reach a steady-state condition $\sim$ 1 minute
- sufficient period to integrate heat-flow signal $\sim$ 5 minutes

Note that the total time to perform a heat-loss measurement using the IR technique could be reduced to 11 minutes, provided a fast heat-flow meter is utilized.

## 6. CONCLUSIONS

A technique for estimating heat-loss was presented that utilizes an IR television system. A device, called a heat-flow reference pad (HFRP), was described which makes it possible to estimate the heat-loss rate at the surface of a building without the need for a conventional heat-flow meter to be mounted on the surface. Technical considerations for the design of a HFRP were presented.

The IR heat-loss measurement technique predicted surface heat-loss rates in the laboratory within approximately 10%. When the front-side heat flux of the HFRP was determined using heat-flow meters as opposed to measuring its electrical power input, the accuracy of the IR heat-loss measurement was improved to approximately 6%. For a final prototype HFRP, it is recommended that the front-side heat flux of the HFRP be measured with a thin heat-flow meter having a small time constant. This would significantly shorten the time required to perform successive adjustments of the HFRP necessary in conducting an IR heat-loss measurement.

In the field the IR heat-loss measurement technique predicted surface heat-loss rates within approximately 12 percent. Outdoor convective air movements caused large fluctuations in the front-side heat-flux rate of the HFRP. It is recommended that the final prototype HFRP use an analog integrator for averaging the signal produced by the heat-flow meter mounted on the HFRP.

A major source of uncertainty in the IR technique for heat-loss measurement is the minimum detectable temperature difference of the IR camera. It was shown that for a 15-mph wind condition, the error due to minimum detectable temperature differences could be as high as 48 percent for an insulated wood-frame wall. However, under still-air conditions, the measurement uncertainty would be less than 12 percent.

An analysis of the error due to differences in the rates of convective heat transfer and surface emissivity at the surfaces of the HFRP and the building surface was performed. It was shown that for the range of emissivities of most common building materials, under still-air conditions, the measurement error would probably be less than 5 percent. However, under windy conditions, a HFRP placed in front of a wall may be more exposed to wind than the wall. It was shown that exposure of the HFRP to a 30-percent greater convective heat-transfer condition under high-wind conditions could result in a measurement error of 19 percent.

The error analysis showed that the most accurate measurements could be attained under still-air conditions. Under such conditions, the net error due to the combination of minimum detectable temperature difference and emissivity would be less than 13 percent.

## 7. REFERENCES

1. Ivar Paljak and Bertil Pettersson, "Thermography of Buildings," Swedish Council of Building Research, Lund Institute of Technology, Lund, Sweden, 1972.

2. Claus G. Bankvall, "Investigation of Temperature and Thermal Insulation by Radiation Measurements," Report 11, Division of Building Technology, Lund Institute of Technology, Lund, Sweden, 1969.

3. R. H. Munis, R. H. Berger, S. J. Marshall, and M. A. Bush, "Detecting Structural Heat-Losses with Mobile Infrared Thermography-Part I Description of Technique - Part II Survey of Pease Air Force Base, Portsmouth, New Hampshire - Part III Survey of USACRREL," Research Reports 326, 338, and 348, Cold Regions Reserach and Engineering Laboratory, Hanover, New Hampshire, 1975.

4. D. M. Burch and C. M. Hunt, "Retrofitting an Existing Wood-Frame Residence for Energy Conservation--An Experimental Study," NBS Report in review.

5. ASTM C 177-71, "Standard Method of Test for Thermal Conductivity of Materials by Means of the Guarded Hot Plate," 1974 Annual Book of ASTM Standards, Part 18, American Society for Testing and Materials.

# APPENDIX

## Technical Considerations for the Design of a Heat-Flow Reference Pad

Technical Considerations for the Design
of a Heat-Flow Reference Pad

## 1. Introduction

The purpose of this section is to provide an analysis of various features which must be considered in the design of a heat-flow reference pad (HFRP).

## 2. Back-Side Losses

An important feature of a heat-flow reference pad is that its back-side heat losses be small, so that most of the power released by the electric heater should appear as front-side heat flux. Under steady-state conditions the fraction of the electric input power ($C_f$) that appears as front-side heat flux is equal to the thermal conductance of the front-side heat-transfer path divided by the sum of the conductances of the front-side and back-side heat-transfer paths, or

$$C_f = \frac{h_f}{h_f + \dfrac{1}{1/h_b + L/k}} \qquad \text{(A-1)}$$

Here $h_f$ and $h_b$ are the front-side and back-side heat-transfer coefficients; L and k are the thickness and thermal conductivity of the insulating board, respectively. This equation assumes one-dimensional steady-state heat transfer. The thermal resistance of the insulating board (L/k) should be selected to be as large as possible, so that the front-side factor ($C_f$) is very nearly unity.

## 3. Uniformity of Front-Side Heat Flux

Another important feature of a HFRP is that it should produce a very uniform front-side heat flux with small edge effects. To analyze the non-uniformity of the front-side heat flux, the heater of the HFRP was replaced with the simplified mathematical model shown in figure A-1. The separate heating elements are replaced with line-source heating elements separated by a distance (d). Heat conduction from the heater into the insulating board is neglected; thus, the back-side surface is treated as adiabatic. Since the heater is very thin, temperature gradients across the heater (perpendicular to the surface of the heater) can be neglected. The rate of heat release for each line-source heating element is denoted by 2m.

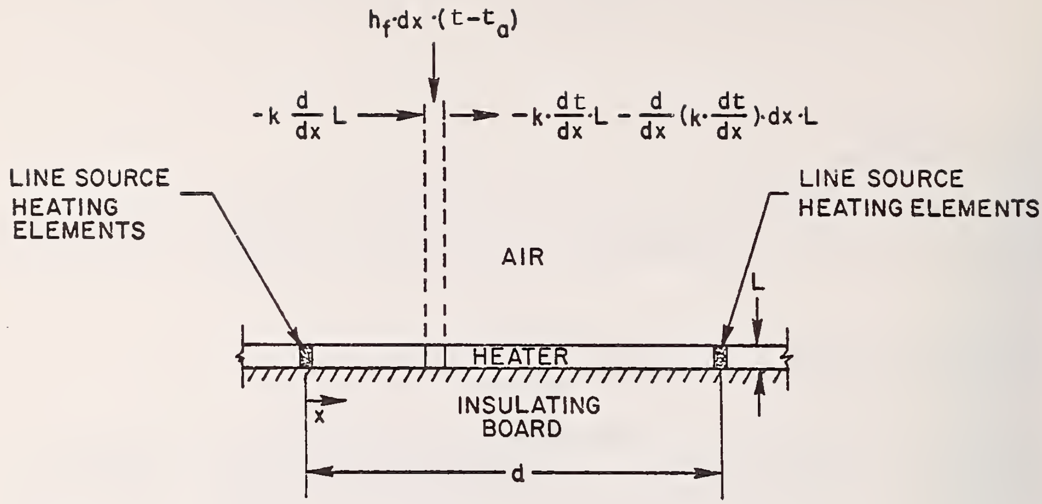


Figure A-1. Simplified mathematical model for thin-foil heater.

When the back-side losses are small, a heat balance on an elemental slice of the fin may be approximated with the second-order differential equation:

$$h_f \cdot (t-t_a) = k \cdot L \cdot \frac{d^2 t}{dx^2} \tag{A-2}$$

The coefficient of heat transfer ($h_f$) is an overall heat-transfer coefficient which includes both the effects of radiation and convection. The foregoing differential equation must satisfy the boundary conditions:

$$L \cdot k \cdot \frac{dt}{dx} = m \quad \text{at} \quad x = 0 \tag{A-3}$$

$$\frac{dt}{dx} = 0 \quad \text{at} \quad x = d/2 \tag{A-4}$$

Introducing the following dimensionless parameters:

$$\eta = x/d, \ \upsilon = (t - t_a)/(m \cdot d/L \cdot k), \text{ and } H = h_f \cdot d^2/k \cdot L)$$

we obtain the dimensionless equations:

$$H\cdot\upsilon = \frac{d^2\upsilon}{d\eta^2} \tag{A-5}$$

$$\frac{d\upsilon}{d\eta} = 0 \quad \text{at} \quad \eta = 1/2 \tag{A-6}$$

$$\frac{d\upsilon}{d\eta} = -1 \quad \text{at} \quad \eta = 0 \tag{A-7}$$

The general solution to (A-5) is

$$\upsilon = A\cdot\cosh(\sqrt{H}\cdot\eta) + B\cdot\sinh(\sqrt{H}\cdot\eta)$$

Application of (A-6) and (A-7) gives

$$\upsilon = \frac{1}{\sqrt{H}}\cdot\frac{\cosh[\sqrt{H}\cdot(1-2\eta)/2]}{\sinh[\sqrt{H}/2]} \tag{A-8}$$

$$\therefore \Delta\upsilon = \upsilon\Big|_{\eta = 0} - \upsilon\Big|_{\eta = \frac{1}{2}} = \frac{1}{\sqrt{H}}\cdot\frac{\cosh\ (\sqrt{H}/2)-1}{\sinh\ (\sqrt{H}/2)} \tag{A-9}$$

As the parameter $(h_f\cdot d^2/k\cdot L)$ becomes small, the temperature difference along the surface becomes very small. This may be accomplished by decreasing the spacing (d) between the separate line-source heating elements and increasing the thermal conductivity of the heater. The thin-foil heater used for the present study has line-source heating elements spaced 0.147 inch on center.

A sample calculation was performed for the thin-foil heater. Taking the overall heat-transfer coefficient to be $h_f$ = 1.46 Btu/h•ft$^2$•F, the thermal conductivity of the heater to be k = 0.233 Btu/h•ft•F, and the thickness of the heater to be L = 0.01225 ft, the maximum temperature variation is found to be Δt = 0.44°F at a front-side heat-flux rate of 3.415 Btu/h•ft$^2$.

The temperature-profile adapter was used to measure the temperature profile across the thin-foil heater of the HFRP. As seen in figure A-2, the temperature is uniform across most of the heater, with the exception

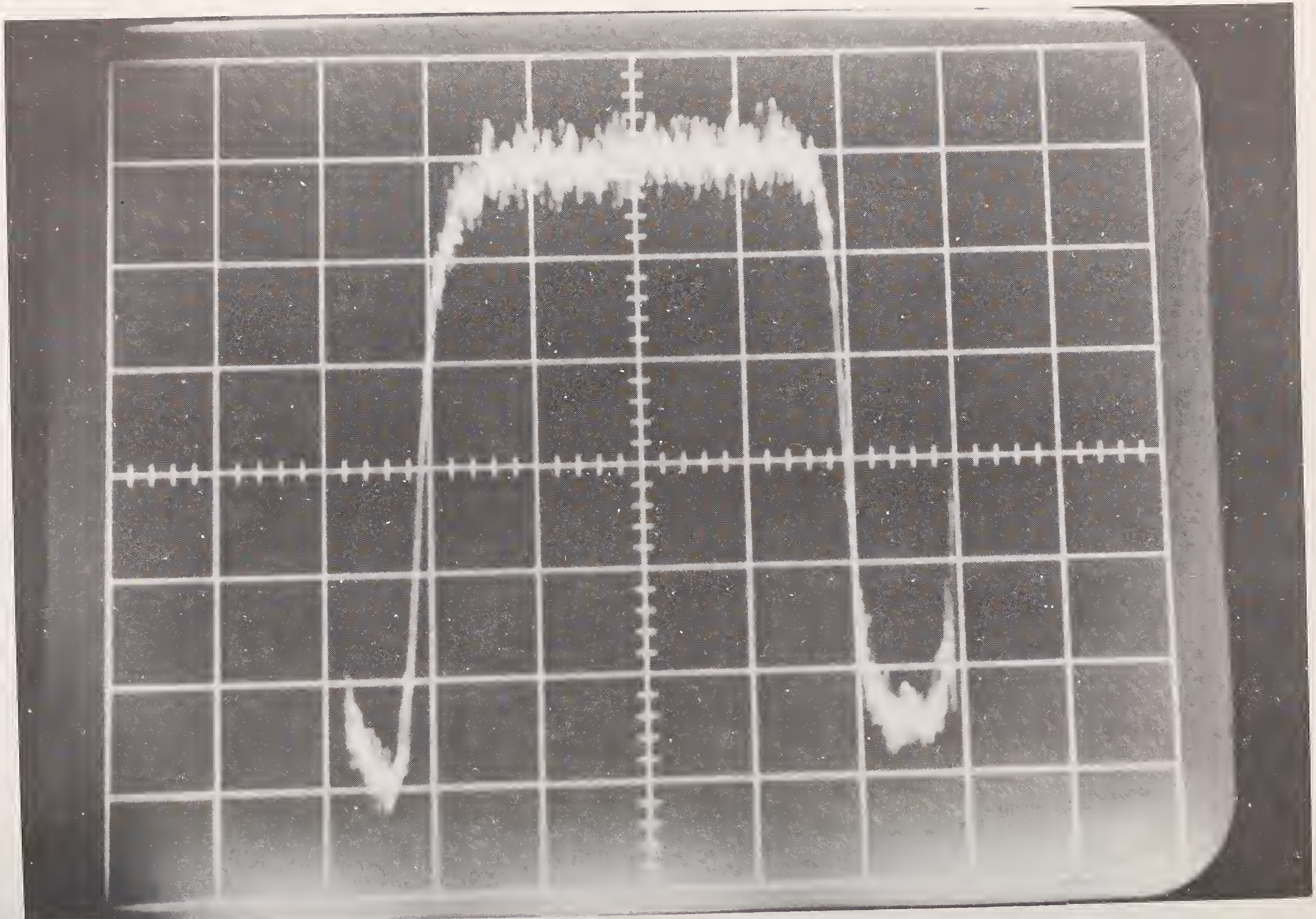

Figure A-2. Temperature variation across HFRP.

of a narrow region at the edges. The temperature variation within the center portion of the profile is seen to be within a 0.36°F temperature band. It should be pointed out that the resolution of the camera is no better than 0.36°F. Since the heat-loss rate at a surface is proportional to the surface-to-air temperature difference, a uniform surface temperature implies a uniform heat-loss rate. Thus, these measurements suggest that a very uniform front-side heat flux is being produced by the HFRP.

## 4. Response Time

Another important feature for a HFRP is that it have a fast response time; that is, very little time be required for the front-side heat flux to reach equilibrium after changing the input power from one level to another. A fast response is desirable so that the successive adjustments required for an IR heat-loss measurement will not be time consuming. For a thin-foil heater mounted on a perfect insulating board, the electric power released by the thin-foil heater must be either lost by convection to the ambient air or stored within the heater. An energy balance of the system results in the following expression:

$$p \cdot A \cdot L - A \cdot h_f \cdot (t - t_a) = A \cdot L \cdot \rho \cdot C_p \cdot \frac{dt}{d\tau} \tag{A-10}$$

where $p$ = heat generation rate per unit volume

$A$ = surface area of the heater

$L$ = thickness of the heater

$t$ = temperature of the heater

$t_a$ = temperature of the ambient air

$h_f$ = overall heat-transfer coefficient

$\rho$ = density of the heater

$C_p$ = specific heat of the heater

$\tau$ = time

Here $h_f$ is the overall heat-transfer coefficient which includes both radiation and convective heat transfer rates. The heater must satisfy the initial condition:

$$t = t_i \text{ for } \tau \leq 0$$

Introducing the following dimensionless parameters :

$$\theta = (t - t_a)/(p \cdot L/h), \ Fo = \tau/((\rho \cdot L \cdot C_p)/h_f), \text{ and } V = (t_i - t_a)/(p \cdot L/h_f)$$

we obtain the dimensionless relations:

$$\frac{d\Theta}{dFo} + \Theta = 1 \tag{A-12}$$

$$\theta = V \text{ for } Fo \leq 0 \tag{A-13}$$

which has the solution:

$$\theta = 1 + (V-1)\cdot e^{-Fo} \tag{A-14}$$

The response of the pad is seen to be a first-order exponential function with a thermal time constant ($\rho \cdot L \cdot C_p/h_f$). The response time can be reduced by decreasing the time constant. This may be accomplished by making the heat capacity per unit area ($\rho \cdot L \cdot C_p$) small. In actual practice, when a thin heater is attached to an insulating board, back-side losses and thermal storage within the insulating board have a significant effect on the response of the HFRP.

The actual response of the experimental-prototype HFRP to a step increase in the rate of electrical-power input is shown in figure A-3. The normalized front-side heat-flux rate ($q/q_f$) is plotted as a function of time in minutes, where $q_f$ is the final steady-state front-side heat-flux rate. The actual response measured with the IR television camera is in good agreement with the theoretical response predicted by equation (A-14) during the first portion of the transient adjustment. After approximately one minute the actual measured response begins to lag behind the theoretical response, due to the back-side losses of the thin-foil heater. The theoretical response as predicted by equation (A-14) treats the insulating board as a perfect insulator; that is, heat transfer into the insulating board is neglected. The sluggish response of the actual HFRP, due to the rather large time required for the back-side losses to reach a steady-state condition, poses a serious problem in determining the front-side heat-flux rate from the rate of electrical-power input to the HFRP.

The measured response determined by the heat-flow meters is also very slow, owing to the rather large time constant of the heat-flow meters. The results of figure A-3 indicate that it is necessary to wait 40 minutes before a steady-state condition is reached. The response may be substantially reduced by using a thin heat-flow meter having a short time constant.

5. HFRP Size Requirements

It is also important that the size of a HFRP be large enough to permit its temperature to be resolved by the IR camera. When attempting to view very small objects with an infrared television system, the level of the video signal obtained for the thermal image of such objects may introduce temperature measurement errors. These errors become significant only when the angle subtended by the object approaches the order of magnitude of the IR camera's instantaneous field-of-view. What happens

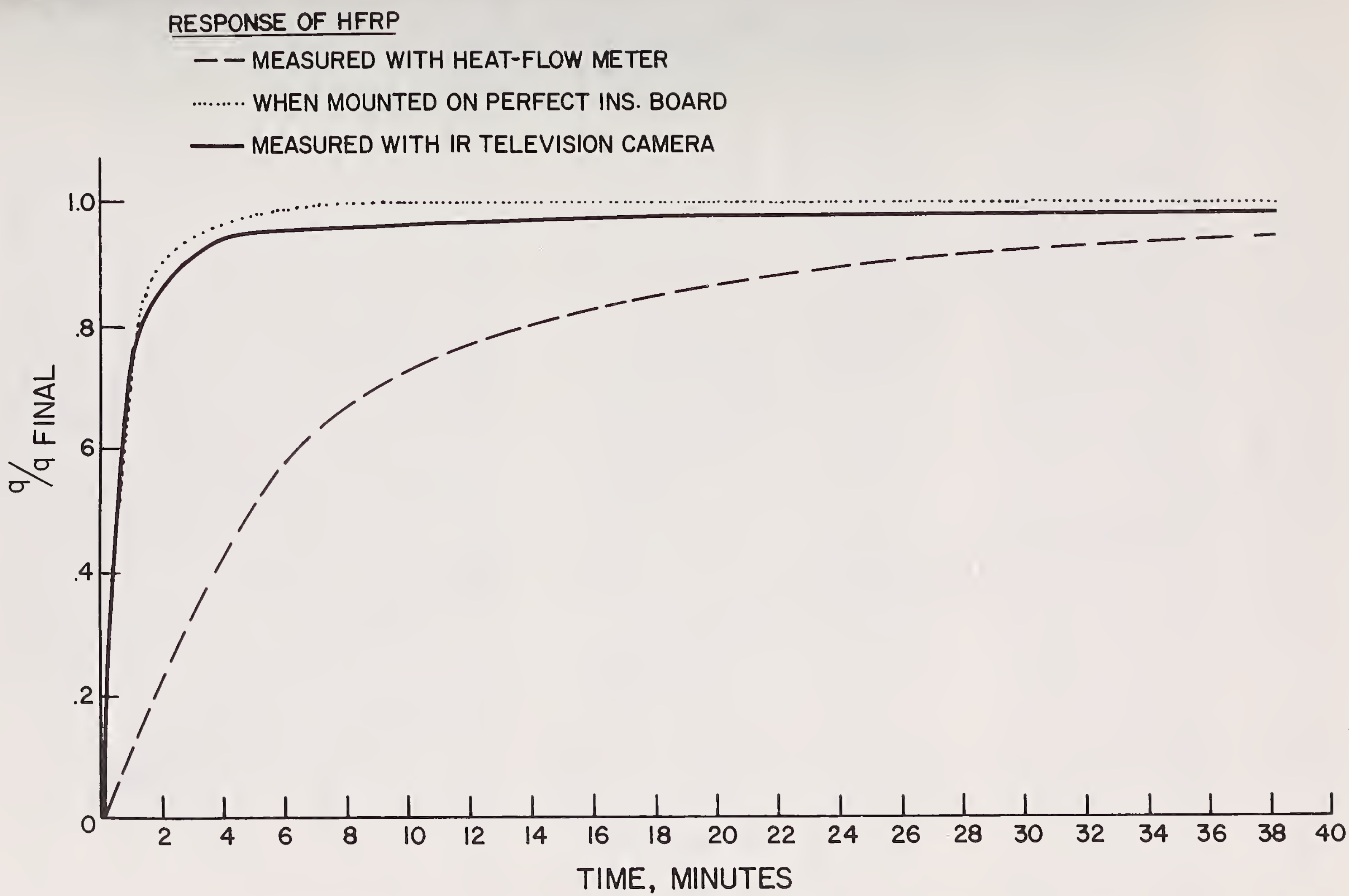


Figure A-3. Response of heat-flow reference pad.

is, the object image size in this case becomes smaller than the IR detector with the result that the detector no longer "sees" only radiation emitted by the object of interest, but also radiation coming from sources supposedly eclipsed by it during the instant of scanning.

Since the detector of the IR camera is square, the instantaneous scanning spot viewed by the detector is also square. Based on information* supplied by the manufacture of the IR camera, the surface temperature of a square-shaped object can be resolved when an edge of the square subtends an angle more than $4.5 \times 10^{-3}$ radians for the 10° field of view lens and more than $11.0 \times 10^{-3}$ radians for the 25° field of view lens. The edge length (s) of the smallest square for which the temperature can be resolved is related to the object distance (r) by the relation:

$$s = x\ r \tag{A-15}$$

where x is the angle subtended by an edge of a square scanning spot. A plot of the minimum size square (expressed in edge length) for which the surface temperature can be resolved as a function of object distance is given in figure A-4. Note that the surface temperature of a 1-ft. square surface can be resolved at 91 feet with the 25° field of view lens.

The above analysis is based on the assumption that a perfect lens and scatter-free scanning system is used. No real optical system is perfect. There is always some blurring of the image due to diffraction. To this must be added the blurring due to aberrations in the lens and scattering at each reflecting or refracting optical surface. Also, since a dynamic scanning system is involved, the time constant of the electronics (detector, amplifier and recorder or display) will make a contribution to the recorded or displayed image.

Assume that a vertical bar of uniform radiance, higher than the radiance of the background by $\Delta L$, is scanned by a noise-free scanner with perfect optics and electronics with a zero time constant. If the band is of a width such that its image exactly fills the detector, the signal produced as its image is scanned across the detector will be two sides of an isosceles triangle, of width equal to twice the width of the detector and the image of the bar, and of height $\Delta L$. With a real system, the image of the bar will be enlarged, because of the blurring at its edges, and the signal produced by a noise-free system of zero time constant will be distorted. The corners of the triangle will be rounded, so that its base is longer, and its peak lower than those of the perfect system. However, the area under the two curves will be the same. When noise is added to the signal, and particularly when the signal-to-noise ratio is low, as it is with the infrared scanner, it becomes very difficult to evaluate the height of the peak. In essence the uncertainty is equal to approximately half the width of the noise band.

---

* AGA Operation Manual for Thermovision System 680, AGA Corporation, 550 County Ave., Secaucus, NJ 07094.


Figure A-4. Minimum size squares for which the surface temperature can be resolved as a function of object distance.

When an area of uniform radiance of width such that its image is twice the width of the detector is scanned, its ideal signal will be in the form of a truncated triangle with a base equal to three times the width of the detector. With a real noise-free system, the signal still has a flat top at a height equivalent to $\Delta L$, of width equal to slightly less than that of the detector. When noise is added to the signal, it can be averaged over the flat peak, and the uncertainty is reduced, by an amount roughly proportioned to the square root of the length of the flat top.

6. Effect of Surface Emissivity and the Rate of Convective Heat Transfer on IR Heat-Loss Measurement

This section presents a theoretical analysis for predicting the error for an IR technique for measuring heat-loss when the emissivity of the surface is different from that of the reference pad, and when the surface and the reference pad are exposed to different rates of convective heat transfer. Several sample problems are then worked out.

The thermal energy ($E_s$)* radiated from a surface is equal to the self-emitted radiation due to the temperature of the surface and reflected thermal radiation from surrounding surfaces, or

$$E_s = \varepsilon_s \cdot \sigma \cdot T_s^4 + (1 - \varepsilon_s) \cdot \varepsilon_a \cdot \sigma \cdot T_a^4 \qquad \text{(A-16)}$$

where $E_s$ = thermal flux radiated from a surface

$\varepsilon_s$ = emissivity of surface

---

* All surfaces are treated as gray bodies which are opaque to infrared radiation.

$T_s$ = absolute temperature of surface

$\varepsilon_a$ = emissivity of surrounding surfaces

$\sigma$ = Stefan-Boltzmann constant

$T_a$ = absolute weighted-average temperature of the surroundings.

Radiation in the visible spectrum has very little energy in the thermal range and will therefore not contribute to the thermal radiation exchange process given by equation (A-16). Similarly, the thermal flux ($E_R$) radiated from a HFRP is given by:

$$E_R = \varepsilon_R \cdot \sigma \cdot T_R^4 + (1 - \varepsilon_R) \cdot \varepsilon_a \cdot \sigma \cdot T_a^4 \qquad \text{(A-17)}$$

In the IR technique for measuring heat loss, both of these surfaces are included in the thermal picture. The difference between the level of video signals for the surface and the HFRP ($\Delta I_{RS}$) is approximately equal to:

$$\Delta I_{RS} \simeq Z \cdot (E_R - E_S) \qquad \text{(A-18)}$$

where Z is the transfer function for the IR television camera.

Substituting equations (A-16) and (A-17) into (A-18) gives

$$\Delta I_{RS} \simeq Z \cdot [\varepsilon_R \cdot \sigma \cdot T_R^4 + (1 - \varepsilon_R) \cdot \varepsilon_a \cdot \sigma \cdot T_a^4$$

$$- \varepsilon_s \cdot \sigma \cdot T_s^4 - (1 - e_s) \cdot \varepsilon_a \cdot \sigma \cdot T_a^4] \qquad \text{(A-19)}$$

Approximating the emissivity of the background to be unity, $\varepsilon_a = 1.0$, and defining $f(T) = Z \cdot \sigma \cdot T^4$, we have that

$$\Delta I_{RS} \simeq \varepsilon_R[f(T_R) - f\ (T_a)] - \varepsilon_s[f(T_s) - f\ (T_a)] \qquad \text{(A-20)}$$

The function f(T) can be determined experimentally and is shown for the IR television camera used for the present study in figure A-5 which can be represented by the relation $f(T) \simeq -86.3 + 0.2 \cdot T$ over the temperature range ($470 \leq T \leq 495$°R or $10 \leq t \leq 35$°F). In the IR technique for measuring heat loss, the reference pad is adjusted so that it has the same radiance temperature as the surface ($\Delta I_{RS} = 0$). Setting $\Delta I_{RS} = 0$, we obtain:

$$f\ (T_R) = \frac{\varepsilon_s}{\varepsilon_R} \cdot f\ (T_s) + (1 - \frac{\varepsilon_s}{\varepsilon_R}) \cdot f\ (T_a) \qquad \text{(A-21)}$$

Substituting the linear relation $f(T) \simeq -86.3 + 0.2 \cdot T$ into equation (A-21), the following relation is obtained:

$$\varepsilon_R \cdot (T_R - T_a) = \varepsilon_s \cdot (T_s - T_a) \qquad \text{(A-22)}$$

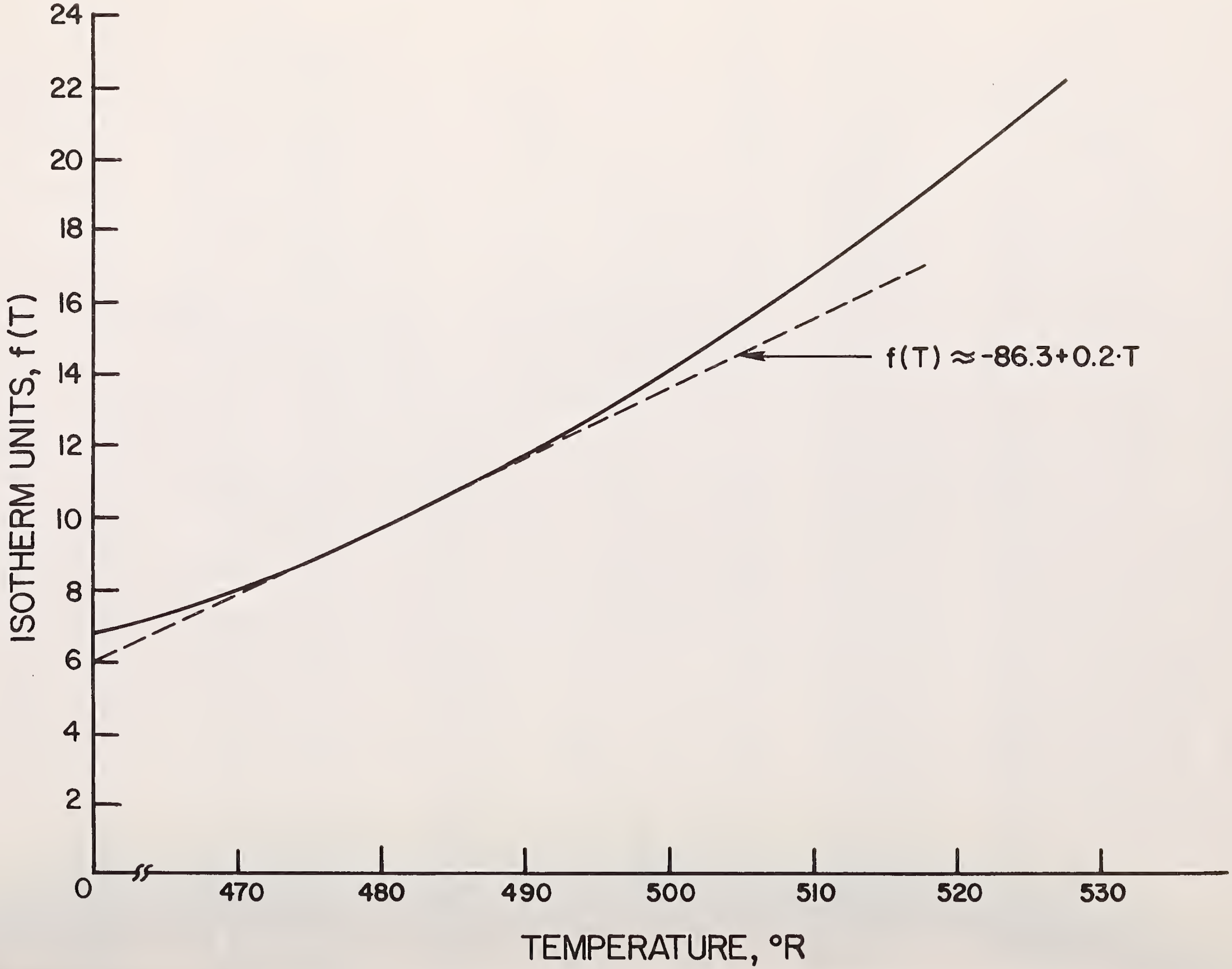


Figure A-5. Function f(T) for IR television camera.

The heat-loss rates from the HFRP and the surface are given by:

$$q_s = \varepsilon_s \cdot \sigma \cdot (T_s^4 - T_a^4) + h_s \cdot (T_s - T_a) \qquad \text{(A-23)}$$

$$q_R = \varepsilon_R \cdot \sigma \cdot (T_R^4 - T_a^4) + h_R \cdot (T_R - T_a) \qquad \text{(A-24)}$$

where $h_s$ and $h_R$ denote the convective heat-transfer coefficient of the surface and the reference pad, respectively. The radiation terms in the foregoing equations may be linearized by noting that

$$\varepsilon_s \cdot \sigma \cdot (T_s^4 - T_a^4) \simeq \varepsilon_s \cdot F \cdot (T_s - T_a) \quad \text{for } T_s \simeq T_a = T \qquad \text{(A-25)}$$

$$\varepsilon_s \cdot \sigma \cdot (T_R^4 - T_a^4) \simeq \varepsilon_s \cdot F \cdot (T_s - T_a) \quad \text{for } T_R \simeq T_a = T \qquad \text{(A-26)}$$

where $F = 4 \cdot \sigma \cdot T^3$. Over the temperature range ($470 \leq T \leq 495°R$ or $10 \leq t \leq 35°F$), F is a weak function of T and may be treated as a constant for the purposes of deriving a simple error expression. Substituting the foregoing linearized radiation terms into equations (A-23) and (A-24) gives

$$q_s = (\varepsilon_s \cdot F + h_s) \cdot (T_s - T_a) \qquad \text{(A-27)}$$

$$q_R = (\varepsilon_R \cdot F + h_R) \cdot (T_R - T_a) \qquad \text{(A-28)}$$

The error is defined by the relation:

$$\text{Error} = \frac{q_s - q_R}{q_s} \qquad \text{(A-29)}$$

Substituting (A-27) and (A-28) into the foregoing equation yields

$$\text{Error} = \frac{(\varepsilon_s \cdot F + h_s) - (\varepsilon_R \cdot F + h_R) \cdot \left(\frac{T_R - T_a}{T_s - T_a}\right)}{\varepsilon_s \cdot F + h_s} \qquad \text{(A-30)}$$

But,

$$\frac{T_R - T_a}{T_s - T_a} = \frac{\varepsilon_s}{\varepsilon_R} \qquad \text{(eq. A-22)}$$

whence,

$$\text{Error} = \frac{h_s/\varepsilon_s - h_r/\varepsilon_R}{h_s/\varepsilon_s + F} = \frac{\Delta(h/\varepsilon)/(h_s/\varepsilon_s)}{1 + F \cdot \varepsilon_s/h_s} \qquad \text{(A-31)}$$

Thus, we see that the error in the infrared technique for measuring heat loss is the percent deviation of the factor ($h/\varepsilon$) for the pad from the corresponding factor ($h/\varepsilon$) for the building surface, divided by the factor ($1 + F \cdot \varepsilon_s/h_s$).

The foregoing error expression is plotted in figure (A-6). This figure shows that the effect of the factor ($h_R/\varepsilon_R$) for the HFRP departing from the factor ($h_s/\varepsilon_s$) for the building surface decreases as the outdoor convective conditions approach a still-air condition. For instance, at approximately a still-air condition ($h_s/\varepsilon_s = 0.5$), when the factor ($h_R/\varepsilon_R$) for the reference pad deviates 10 percent from the value for the building surface, the error is only 3 percent. However, at approximately a 15-mph wind condition the same deviation produces an error of 8.7 percent. This analysis clearly indicates that the optimum outdoor condition for which the most accurate heat-loss measurements can be performed are still-air conditions.

Perhaps the most crucial issue that needs to be addressed is the typical accuracy that one might expect to achieve in performing a field measurement. To assist in several sample calculations, infrared emissivities for various building surfaces and paints are given in tables A-1 and A-2, respectively.* Several sample calculations are given in the following example:

Consider an exterior wood-frame wall shown in figure A-7. Take the outdoor temperature to be $10^{o}$ F. The percent error is calculated below for still air and 15-mph conditions for cases in which the emissivities of the building surface are 0.90 and 0.85. The emissivity at the surface of the HFRP is taken to be 0.96.

Still-air conditions

For still-air conditions, it is very likely that the heat-transfer coefficients at the building surface and the HFRP would be very nearly the same. Hence, $h_R = h_s = 0.5$.

1. For the case $\varepsilon_s = 0.90$

$h_s/\varepsilon_s = 0.5/0.90 = .556$

$h_R/\varepsilon_R = 0.5/0.96 = .521$

$\Delta(h/\varepsilon)/(h_s/\varepsilon_s) = .063$

Error = 2.5% (figure A-6)

* See pages A-22, A-23, A-24.

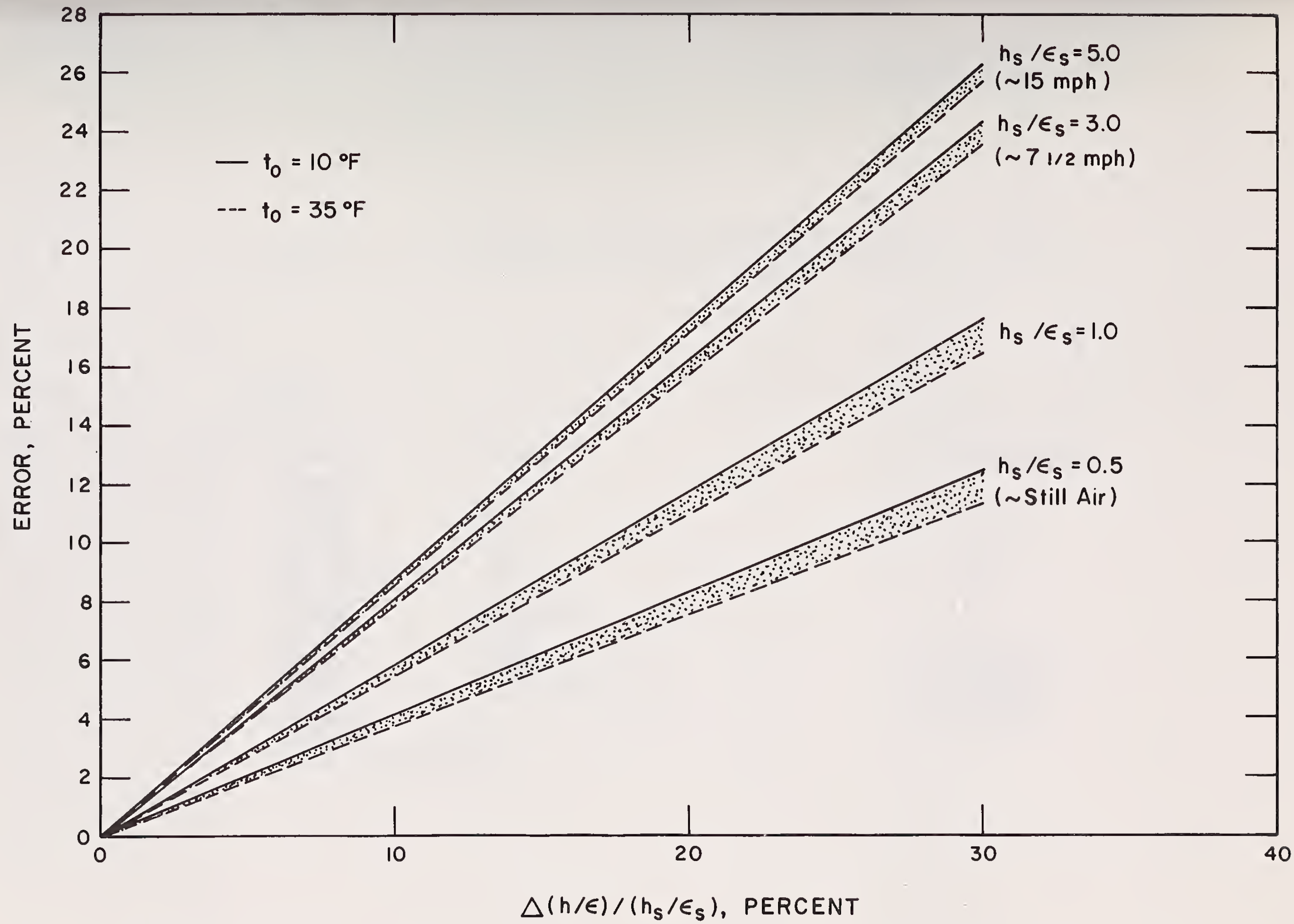


Figure A-6. The effect of surface emissivity and surface convective heat transfer on the error of infrared technique for measuring heat loss.

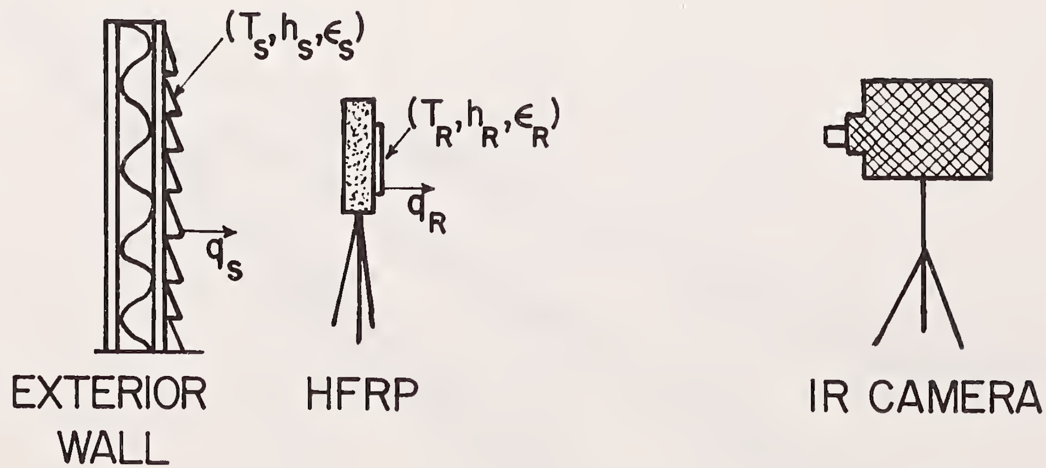


Figure A-7. IR technique being used to measure heat-loss rate from exterior wood-frame wall.

2. <u>For the case $\varepsilon_s = 0.85$</u>

$h_s/\varepsilon_s = 0.5/0.85 = .588$

$h_R/\varepsilon_R = 0.5/0.96 = .521$

$\Delta(h/\varepsilon)/(h_s/\varepsilon_s) = .114$

Error = 4.7% (figure A-6)

<u>15-mph condition</u>

For this sample calculation, it shall be assumed that the HFRP is in a more exposed condition. The heat-transfer coefficient at the surface of the HFRP will be taken to be 30 percent higher than the value at the surface of the building. Therefore, $h_s = 1.3(5) = 6.5$ Btu/h·ft$^2$·F.

1. <u>For the case $\varepsilon_s = 0.9$</u>

$h_s/\varepsilon_s = 5.0/0.9 = 5.56$

$h_R/\varepsilon_R = 6.5/0.96 = 6.77$

$\Delta(h/\varepsilon)/(h_s/\varepsilon_s) = -.218$

Error = −19.1% (figure A-6)

2. <u>For the case $\varepsilon_s = 0.85$</u>

$h_s/\varepsilon_s = 5.0/0.85 = 5.88$

$h_R/\varepsilon_R = 6.5/0.96 = 6.77$

$\Delta(h/\varepsilon)/(h_s/\varepsilon_s) = -.151$

Error = −13.3% (figure A-6)

The foregoing sample calculations suggest that, when the infrared technique is used to perform heat-loss measurements under still-air conditions, the error will be quite small and will probably be less than 5 percent. On the other hand, when measurements are performed under high-wind conditions, precautions need to be taken to insure that both the building surface and the HFRP are exposed to the same convective conditions, in order to obtain accurate measurements. It was shown that exposure of the HFRP to 30 percent greater convective heat-transfer conditions could result in a measurement error of 19 percent.

7. Errors in the IR Technique for Heat-Loss Measurement Due to the Minimum Detectable Temperature Difference of the IR Camera.

As the surface temperature of an object is reduced, the amount of radiated energy is reduced. The minimum temperature difference which can be detected by an IR television camera depends on the ratio $\Delta E/\Delta T$, where $\Delta E$ is the change in radiated energy and $\Delta T$ is the change in object temperature. Over the spectral range for the IR camera, 2 to 5.6 μm, the ratio ($\Delta E/\Delta T$) decreases as the object temperature decreases. Therefore, the minimum temperature difference which can be detected by an IR camera increases as the object temperature decreases. A plot of the minimum detectable temperature difference for the IR camera used for the present study as a function of object temperature is given in figure A-8.

The accuracy of the IR technique for heat-loss measurement strongly depends on the precision to which the radiance temperature level of the HFRP can be adjusted to the level for a building surface. The uncertainty in performing this adjustment will in turn depend on the minimum detectable temperature difference.

When the emittance and rate of convective heat transfer for the HFRP and the surface of a building are identical ($h_R = h_s$ and $e_R = e_s$), the expression for error given by eq. A-30 reduces to:

$$\text{Error} = \frac{T_s - T_R}{T_s - T_a} = \Delta T_m/(T_s - T_a) \qquad \text{(A-32)}$$

where $\Delta T_m$ is the minimum detectable temperature difference for the IR camera and ($T_s - T_a$) is the temperature difference between the building surface and the ambient outdoor air.

Under steady-state conditions, the heat-flux rate (q/A) through a wall is governed by the relation:

$$q/A = U \cdot (T_i - T_a) = h \cdot (T_s - T_a) \qquad \text{(A-33)}$$

where U = thermal transmittance of the building component

h = overall heat-transfer coefficient

$T_i - T_a$ = air-to-air temperature difference across the building component

$T_s - T_a$ = surface-to-air temperature difference.

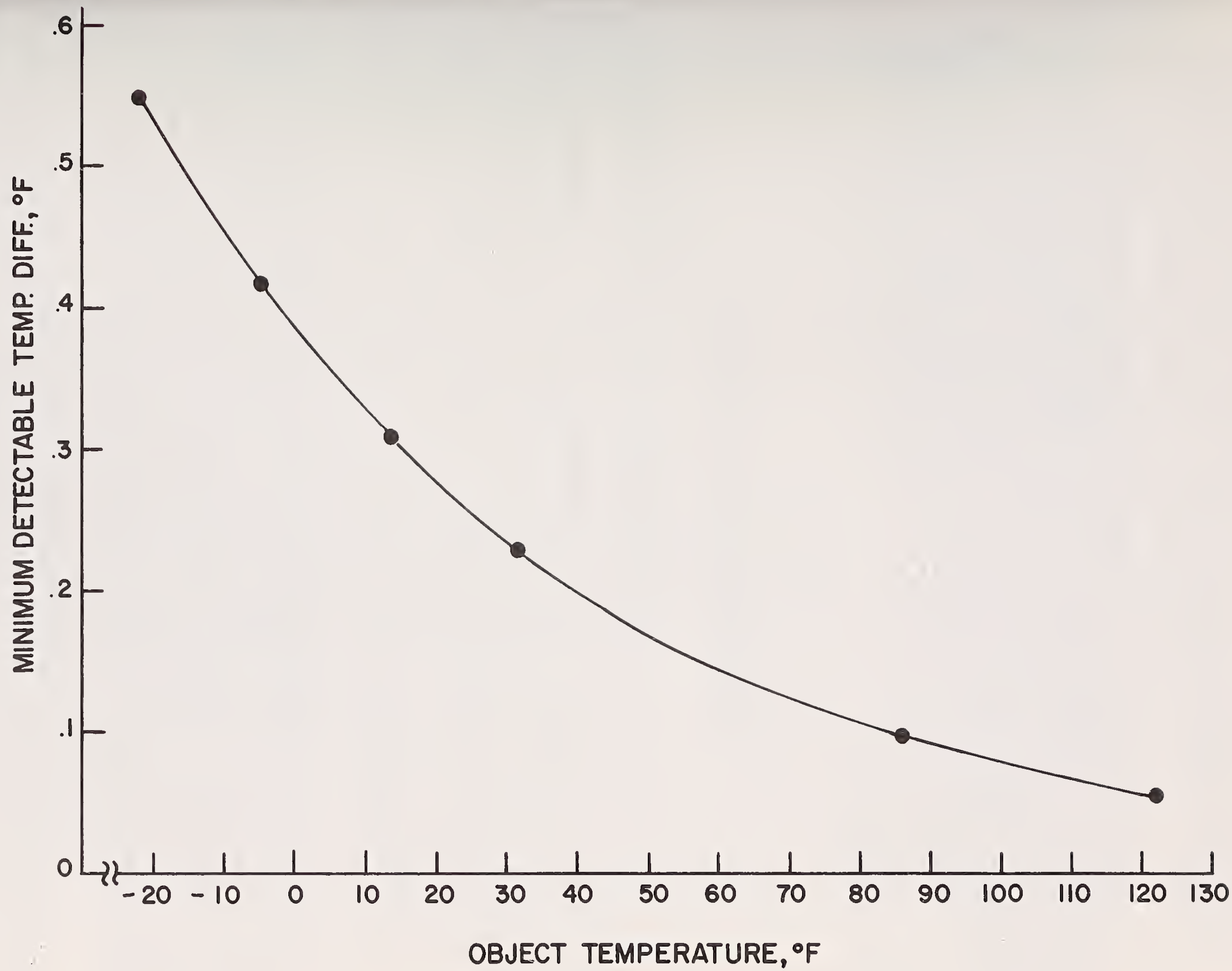


Figure A-8. Minimum detectable temperature difference as a function of object temperature.

Introducing equation (A-33) into (A-32) gives

$$\text{Error} = \Delta T_m \cdot h/U \cdot (T_i - T_a) \qquad \text{(A-34)}$$

The crucial issue to be examined is the amount of measurement error due to minimum detectable temperature difference that occurs in typical applications. Measurement error due to minimum detectable temperature difference is investigated for an uninsulated wood-frame wall ($U = 0.2$ $Btu/h \cdot ft^2 \cdot F$) and an insulated wood-frame wall ($U = 0.065$ $Btu/h \cdot ft^2 \cdot F$). Measurement errors were calculated for these two walls using equation A-34 for still-air conditions ($h = 1.46$ $Btu/h \cdot ft^2 \cdot F$) and 15-mph wind conditions ($h = 6.0$ $Btu/h \cdot ft^2 \cdot F$). For these calculations, the temperature of the indoor air was taken to be 75°F. Calculations were performed for outdoor air temperatures of 32°F and 0°F. The results of these calculations are given in table A-3.

Table A-3.

Measurement Errors Due to Miniumum Detectable Temperature Difference

| Description of Wall | Still-Air Condition ($h = 1.46$ $Btu/h \cdot ft^2 \cdot F$) Temperature, °F | | 15-mph Condition $h = 6.0$ $Btu/h \cdot ft^2 \cdot F$ Temperature, °F | |
|---|---|---|---|---|
| | 32 | 0 | 32 | 0 |
| Insulated wall ($U = 0.065$ $Btu/h \cdot ft^2 \cdot F$) | 11.7 | 11.4 | 48.3 | 46.7 |
| Non-insulated wall ($U = 0.2$ $Btu/h \cdot ft^2 \cdot F$) | 3.8 | 3.7 | 15.7 | 15.2 |

The results dramatically illustrate that measurement error due to the minimum detectable temperature difference of the IR camera increases substantially as the rate of convective heat transfer at the surfaces of the HFRP and the building increase. This is due to the fact that the surface-to-air temperature difference decreases as the rate of convective heat transfer increases. Also, the IR technique can more accurately measure heat-loss rate for non-insulated walls than for insulated walls. Again, this finding is due to the fact that the surface-to-air temperature difference decreases as the heat-loss rate decreases.

It was pointed out during the review of this paper that the infrared television system used for the study could have been modified to permit distinction of much smaller temperature differences. One way of accomplishing

this would have been to specially process the video signal of the single trace line displayed on the cathode-ray tube of the temperature profile adaptor. By averaging the signal from various portions of the trace line, the signal-to-noise ratio could have been enhanced, permitting smaller difference in signal level to be detected. However, such modifications were beyond the scope of the present study.

The error analysis presented in the last two sections showed that much more accurate measurements could be attained under still-air conditions, it was shown that an upper limit on the error due to emissivity was 5 percent and the error due to minimum detectable temperature difference was 12 percent. The net error due to the combination of these sources is given by the square root of the sum of the squares of the separate error sources. Thus, the net error due to these sources under still-air conditions is 13 percent.

TABLE A-1

Infrared Emissivities of Common Building Surfaces

| Building Surface | Emissivity: Total Normal $\varepsilon_n$(°F) | Ref. | Emissivity: Hemispherical $\varepsilon_h$(°F) | Ref. |
|---|---|---|---|---|
| BRICK | | | | |
| Brick wall | .94 (68) | 1 | | |
| red rough | .93 (70) | 2 | 0.93-0.95(32-392) | 5 |
| type not specified | | | 0.93(70) | 6 |
| | | | 0.96(68) | 3 |
| red | | | 0.93(32-199) | 4 |
| WOOD | | | | |
| type not specified | .80-0.9(68) | 1 | | |
| sanded spruce | | | 0.82(199) | 7 |
| oak, planed | 0.91(100) | 2 | .895(32-199) | 8 |
| | | | .89(32-392) | 5 |
| | | | .895(70) | 2 |
| CONCRETE | | | | |
| rough | | | 0.94(32-199) | 4 |
| PLASTERING MATERIALS | | | | |
| Gypsum | 0.9(100) | 2 | | |
| Plaster, rough lime | 0.8-0.9(68) | 1 | | |
| | 0.91(100) | 9 | 0.91(50-190) | 9 |
| Plaster | 0.93(100) | 2 | 0.91(32-392) | 5 |
| Plaster, rough | | | 0.91(32-199) | 8 |
| GLASS | | | | |
| type not specified | 0.9(100) | 10 | | |
| polished | 0.94(68) | 1 | | |
| MISCELLANEOUS | | | | |
| roofing paper | 0.91(68) | 1 | 0.91(70) | 2 |

TABLE A-2

Infrared Emissivities of Common Paints

| | Emissivity | | | |
|---|---|---|---|---|
| | Total Normal | | Hemispherical | |
| Type Paint | $\varepsilon_n$(°F) | Ref. | $\varepsilon_h$(°F) | Ref. |
| OILS | | | | |
| type not specified | .89-.97(68) | 1 | | |
| 16 different colors | | | .92-.96 (212) | 10 |
| all colors | | | .92-.96 (32-199) | 8 |
| ENAMELS | | | | |
| white | .92(125) | 2 | | |
| camouflage green | .85(125) | 11 | | |
| green | .82(125) | 11 | | |
| LACQUER | | | | |
| flat black | .96(125) | 12 | | |
| black | | | .96(199) | 7 |
| white | .925(212) | 13 | .95(68) | 14 |
| matt black | .97(176) | 13 | | |
| ALUMINUM | | | | |
| all types | .27-0.60 | 15 | .4-.7(0-100) | 17 |
| | | | .3-.5(68) | 16 |

1. D'Ans, J. and Ellen Lax, "Taschenbuch fur Chemiker and Physiker," Springer - Verlag, Berlin (1943).

2. Schmidt, E., Gesundheite - Ingenier, 20, (1), 1-23 (1927).

3. Randerson, H. Y., "Australian Sanitary Engineering Practice," 3-d Ed. Angus and Robertson, Sydney, (1949).

4. Forsythe, W. E. and Worthing, A. G., "Properties of Tungsten -W- and Characteristics of Tungsten Lamps" Astrophysical Journal, 61:146-185 (1925).

5. Cammerer, J. S. "The Thermal Properties of Wood and Materials Containing Wood, "Holz als rohund Wenkstoff, 1(6): 206-213 (1938).

6. Grant, G. R. "Design of Simple Shelter from the Sun. The Role of Emissivity and Graphs to Facilitate the Use of Available Data," University of Queensland Interim Report No. 1, Project 103, (1949) (Mimeo).

7. McDermott, P. F., "An Apparatus for Measurement of the Total Emissivity of Sheet-Materials in the Temperature-Range 140-500F." Review of Scientific Instruments, 8, (6), 185-192 (1937).

8. Anon. "Heat Transmission and Radiation," Heating and Ventilating, 43, 72a-72b, (1946).

9. Wamsler, F., Feitschr, Ver. Deutsch. Ing. 55, 599 (1911).

10. McAdams, W. H., "Heat Trans-transmission" quoted from Standard Oil Development Company (Personal Communication to H. C. Hottel, 1928) 4-d Ed., p 393-396, McGraw Hill, New York and London (1942).

11. Boelter, Bromberg, and Gier. (N.A.C.A. Wartime Report, 19. An Investigation of Aircraft Heaters. Part XV. The Emissivity of Several Materials. University of California (1944).

12. Hluika, F., Annal .d. Physik, 96, 230 (1933).

13. Eckert, E., "Introduction to Transfer of Heat and Mass," McGraw Hill Book Co., First Edition (1950).

14. Littleton, J. T. Jr., Phys. Rev., 33, 453 (1911).

15. Standard Oil Development Company, Personal Communication (1928).

16. Allcut, E. A. "The Use of Heat Insulation in Building - Design and Instruction," Royal Architectural Institute of Canada, Journal, 24 90-100, (1947).

17. Fishenden, M. and Saunders, O. A., Introduction to Heat Transfer, Clarendon Press, London (1950).

NBS-114A (REV. 7-73)

| U.S. DEPT. OF COMM. BIBLIOGRAPHIC DATA SHEET | 1. PUBLICATION OR REPORT NO. NBS TN-933 | 2. Gov't Accession No. | 3. Recipient's Accession No. |
|---|---|---|---|
| 4. TITLE AND SUBTITLE<br>AN INFRARED TECHNIQUE FOR HEAT-LOSS MEASUREMENT | | | 5. Publication Date<br>April 1977 |
| | | | 6. Performing Organization Code |
| 7. AUTHOR(S) D.M. Burch, T. Kusuda, and D.G. Blum | | | 8. Performing Organ. Report No. |
| 9. PERFORMING ORGANIZATION NAME AND ADDRESS<br>NATIONAL BUREAU OF STANDARDS<br>DEPARTMENT OF COMMERCE<br>WASHINGTON, D.C. 20234 | | | 10. Project/Task/Work Unit No.<br>462 6417 |
| | | | 11. Contract/Grant No. |
| 12. Sponsoring Organization Name and Complete Address *(Street, City, State, ZIP)*<br>Federal Energy Administration<br>Washington, D.C. 20461 | | | 13. Type of Report & Period Covered<br>Final |
| | | | 14. Sponsoring Agency Code |

15. SUPPLEMENTARY NOTES

16. ABSTRACT *(A 200-word or less factual summary of most significant information. If document includes a significant bibliography or literature survey, mention it here.)*


This paper describes a newly developed technique for measuring heat-loss rate utilizing an infrared television system. A device called a heat-flow reference pad was developed that makes it possible to measure quantitatively the heat-loss rate through the surface of a building without the need for a conventional heat-flow meter to be mounted on the surface. Technical considerations for the design of a heat-flow reference pad are presented. The infrared measurement technique predicted heat-loss rates in the laboratory and field within approximately 12%.


17. KEY WORDS *(six to twelve entries; alphabetical order; capitalize only the first letter of the first key word unless a proper name; separated by semicolons)*

Heat-flow measurements; infrared heat-loss measurement technique; measurement technology; thermography.

| 18. AVAILABILITY [X] Unlimited | 19. SECURITY CLASS (THIS REPORT)<br>UNCLASSIFIED | 21. NO. OF PAGES<br>52 |
|---|---|---|
| [ ] For Official Distribution. Do Not Release to NTIS<br>[X] Order From Sup. of Doc., U.S. Government Printing Office Washington, D.C. 20402, SD Cat. No. C13.46:933<br>[ ] Order From National Technical Information Service (NTIS) Springfield, Virginia 22151 | 20. SECURITY CLASS (THIS PAGE)<br>UNCLASSIFIED | 22. Price $1.10 |

USCOMM-DC 29042-P74

☆ U.S. GOVERNMENT PRINTING OFFICE : 1977--240-848/40

# NBS TECHNICAL PUBLICATIONS

## PERIODICALS

**JOURNAL OF RESEARCH** reports National Bureau of Standards research and development in physics, mathematics, and chemistry. It is published in two sections, available separately:

• **Physics and Chemistry (Section A)**
Papers of interest primarily to scientists working in these fields. This section covers a broad range of physical and chemical research, with major emphasis on standards of physical measurement, fundamental constants, and properties of matter. Issued six times a year. Annual subscription: Domestic, $17.00; Foreign, $21.25.

• **Mathematical Sciences (Section B)**
Studies and compilations designed mainly for the mathematician and theoretical physicist. Topics in mathematical statistics, theory of experiment design, numerical analysis, theoretical physics and chemistry, logical design and programming of computers and computer systems. Short numerical tables. Issued quarterly. Annual subscription: Domestic, $9.00; Foreign, $11.25.

**DIMENSIONS/NBS (formerly Technical News Bulletin)**—This monthly magazine is published to inform scientists, engineers, businessmen, industry, teachers, students, and consumers of the latest advances in science and technology, with primary emphasis on the work at NBS. The magazine highlights and reviews such issues as energy research, fire protection, building technology, metric conversion, pollution abatement, health and safety, and consumer product performance. In addition, it reports the results of Bureau programs in measurement standards and techniques, properties of matter and materials, engineering standards and services, instrumentation, and automatic data processing.

Annual subscription: Domestic, $12.50; Foreign, $15.65.

## NONPERIODICALS

**Monographs**—Major contributions to the technical literature on various subjects related to the Bureau's scientific and technical activities.

**Handbooks**—Recommended codes of engineering and industrial practice (including safety codes) developed in cooperation with interested industries, professional organizations, and regulatory bodies.

**Special Publications**—Include proceedings of conferences sponsored by NBS, NBS annual reports, and other special publications appropriate to this grouping such as wall charts, pocket cards, and bibliographies.

**Applied Mathematics Series**—Mathematical tables, manuals, and studies of special interest to physicists, engineers, chemists, biologists, mathematicians, computer programmers, and others engaged in scientific and technical work.

**National Standard Reference Data Series**—Provides quantitative data on the physical and chemical properties of materials, compiled from the world's literature and critically evaluated. Developed under a world-wide program coordinated by NBS. Program under authority of National Standard Data Act (Public Law 90-396).

NOTE: At present the principal publication outlet for these data is the Journal of Physical and Chemical Reference Data (JPCRD) published quarterly for NBS by the American Chemical Society (ACS) and the American Institute of Physics (AIP). Subscriptions, reprints, and supplements available from ACS, 1155 Sixteenth St. N.W., Wash. D. C. 20056.

**Building Science Series**—Disseminates technical information developed at the Bureau on building materials, components, systems, and whole structures. The series presents research results, test methods, and performance criteria related to the structural and environmental functions and the durability and safety characteristics of building elements and systems.

**Technical Notes**—Studies or reports which are complete in themselves but restrictive in their treatment of a subject. Analogous to monographs but not so comprehensive in scope or definitive in treatment of the subject area. Often serve as a vehicle for final reports of work performed at NBS under the sponsorship of other government agencies.

**Voluntary Product Standards**—Developed under procedures published by the Department of Commerce in Part 10, Title 15, of the Code of Federal Regulations. The purpose of the standards is to establish nationally recognized requirements for products, and to provide all concerned interests with a basis for common understanding of the characteristics of the products. NBS administers this program as a supplement to the activities of the private sector standardizing organizations.

**Consumer Information Series**—Practical information, based on NBS research and experience, covering areas of interest to the consumer. Easily understandable language and illustrations provide useful background knowledge for shopping in today's technological marketplace.

*Order* **above** *NBS publications from: Superintendent of Documents, Government Printing Office, Washington, D.C. 20402.*

*Order* **following** *NBS publications—NBSIR's and FIPS from the National Technical Information Services, Springfield, Va. 22161.*

**Federal Information Processing Standards Publications (FIPS PUBS)**—Publications in this series collectively constitute the Federal Information Processing Standards Register. Register serves as the official source of information in the Federal Government regarding standards issued by NBS pursuant to the Federal Property and Administrative Services Act of 1949 as amended, Public Law 89-306 (79 Stat. 1127), and as implemented by Executive Order 11717 (38 FR 12315, dated May 11, 1973) and Part 6 of Title 15 CFR (Code of Federal Regulations).

**NBS Interagency Reports (NBSIR)**—A special series of interim or final reports on work performed by NBS for outside sponsors (both government and non-government). In general, initial distribution is handled by the sponsor; public distribution is by the National Technical Information Services (Springfield, Va. 22161) in paper copy or microfiche form.

## BIBLIOGRAPHIC SUBSCRIPTION SERVICES

**The following current-awareness and literature-survey bibliographies are issued periodically by the Bureau:**

**Cryogenic Data Center Current Awareness Service.** A literature survey issued biweekly. Annual subscription: Domestic, $20.00; Foreign, $25.00.

**Liquified Natural Gas.** A literature survey issued quarterly. Annual subscription: $20.00.

**Superconducting Devices and Materials.** A literature survey issued quarterly. Annual subscription: $20.00. Send subscription orders and remittances for the preceding bibliographic services to National Bureau of Standards, Cryogenic Data Center (275.02) Boulder, Colorado 80302.

U.S. DEPARTMENT OF COMMERCE
National Bureau of Standards
Washington, D.C. 20234

OFFICIAL BUSINESS

Penalty for Private Use, $300

POSTAGE AND FEES PAID
U.S. DEPARTMENT OF COMMERCE
COM-215

U.S.MAIL

SPECIAL FOURTH-CLASS RATE
BOOK